TABLE 1. Selected proteins that reproducibly increased in the DRM fraction of SGR-N cells[a]

Avg ratio	*P* (Student *t* test)	Coverage (%)	Protein name	Molecular function	GI no.
5.56	0.04	27	GRP94	Protein folding	15010550
4.99	0.07	47	Hsp60	Protein folding	6996447
3.73	0.07	6	tRNA guanine transglycosylase	Metabolism	30583205
3.56	0.06	23	KIAA0088	Unknown	577295
3.32	0.07	4	Thioredoxin-related protein	Unknown	20067392
3.32	0.13	12	Tat binding protein 1 (TBP-1)	Cellular processes	20532406
3.06	0.14	22	Aldehyde dehydrogenase 1	Metabolism	2183299
3.06	0.14	14	Chaperonin TRiC/CCT, subunit 2	Protein folding	54696794
2.96	0.04	14	Heat shock 70-kDa protein 4 (HSPA4)	Protein folding	6226869
2.96	0.04	29	GRP58	Metabolism/protein folding	2245365
2.94	0.01	37	Mutant β-actin	Cytoskeleton organization	28336
2.65	0.17	33	Glutathione S-transferase (GST)	Catalytic activity	2204207
2.53	0.04	37	Keratin 19	Cytoskeleton organization	6729681
2.46	0.08	6	Heterogeneous nuclear ribonucleoprotein K	Nucleic acid modification	460789
2.45	0.001	13	HMG-coenzyme A synthase	Metabolism	30009
2.4	0.02	31	CKB	Energy pathway/metabolism	180570
2.4	0.02	11	Cathepsin D	Cellular processes	30582659
2.4	0.02	11	C8orf2	Unknown	37181322
2.36	0.1	38	Tropomyosin 4-anaplastic lymphoma kinase fusion protein	Cytoskeleton organization	14010354
2.36	0.1	6	Calreticulin	Protein folding	30583735
2.33	0.01	29	Quinolinate phosphoribosyltransferase	Metabolism	30583301
2.29	0.04	25	Protein disulfide isomerase-related protein 5	Protein folding	1710248
2.29	0.04	16	Tat binding protein 7 (TBP-7)	Cellular processes	263099
2.05	0.11	24	Calumenin	Metabolism	2809324
2.05	0.12	10	TRiC/CCT, subunit 5	Protein folding	24307939
2.03	0.07	20	Hsp90 beta	Protein folding	34304590
2.01	0.07	10	TRiC/CCT, subunit 1	Protein folding	36796

[a] The spectra obtained by tandem mass spectrometry were collected using data-dependent mode, and the results were subjected to database (NCBInr) search by Mascot server software (Matrix Science, London, United Kingdom) for peptide assignment. Coverage, the ratio of the portion of protein sequence covered by matched peptides to the whole protein sequence. GI no., GenInfo identifier number.

genes examined, we observed a reproducible inhibition of HCV RNA replication by two independent siRNAs targeting CKB (see below).

CKB participates in HCV RNA replication and the propagation of infectious virus. CKB is a brain-type creatine kinase isoenzyme and is also detected in a variety of other tissues, including human liver (32). Steady-state levels of CKB in the DRM fraction, as well as in whole-cell lysate of SGR-N cells were compared to those from parental cells by Western blotting. The CKB level in the DRM fraction of replicon cells was higher than that in parental cells (Fig. 1E), confirming the results of the proteome analysis described above. In contrast, the CKB level in whole cells was similar in both cells (Fig. 1E). These results suggest participation of posttranslational modification, such as translocation to the DRM fraction, of CKB in replicon cells.

Figure 2A shows the inhibitory effect on HCV RNA replication of CKB siRNA; siCKB-2, the sequence of which does not overlap with the sequence of siCKB-1 used in the above siRNA screening (Fig. 1D). Transfection with siCKB-2 effectively decreased the cellular level of CKB enzymatic activity (data not shown), as well as the abundance of CKB protein (Fig. 2A), and resulted in 60% reduction in the viral RNA level in SGR-N cells compared to the cells treated with control siRNA. This inhibitory effect of siRNA on HCV RNA abundance was also observed in JFH-1-derived subgenomic replicon (SGR-JFH1) cells. The viral RNA level in the cells transfected with siCKB-2 decreased by 50% compared to the control (Fig. 2A). We also tested the CKB mutant, CKB-C283S, in which Cys at aa 283, near the catalytic site, has been replaced with Ser (Fig. 3A) and which is known to be enzymatically inactive and to work in a dominant-negative manner (22, 29). As expected, overexpression of CKB-C283S resulted in a reduction in HCV RNA replication in SGR-N cells (Fig. 2B). We obtained a similar result in SGR-JFH1 cells, as described below (Fig. 3E).

To further examine the involvement of CKB in HCV RNA replication, we tested the effect of Ccr, a substrate analogue and possible inhibitor for CK in either SGR-N, SGR-JFH1 (Fig. 2C), or Huh7 cells transiently replicating luciferase-subgenomic replicon (data not shown). We found dose-dependent inhibition of HCV RNA replication but no observed effect on total cellular levels of protein and ATP (Fig. 2D) in the replicon setting used.

We next examined whether the knockdown of CKB or treatment with Ccr would abrogate the production of HCVcc. At 72 h posttransfection with siCKB-2, the HCV core level in cells infected with HCVcc was significantly reduced (Fig. 2E). Treatment of the infected cells with Ccr at various concentrations also reduced the intracellular and supernatant core level and subsequently decreased HCVcc production (Fig. 2F). These results demonstrate that suppression of the HCV RNA replication by the siRNA-mediated knockdown of CKB or treatment with CKB inhibitor leads to reduction of the production of infectious virus.

CKB interacts with HCV NS4A. Having established a role for CKB in HCV RNA replication, we then tried to determine to how CKB influences the HCV life cycle. It has been re-

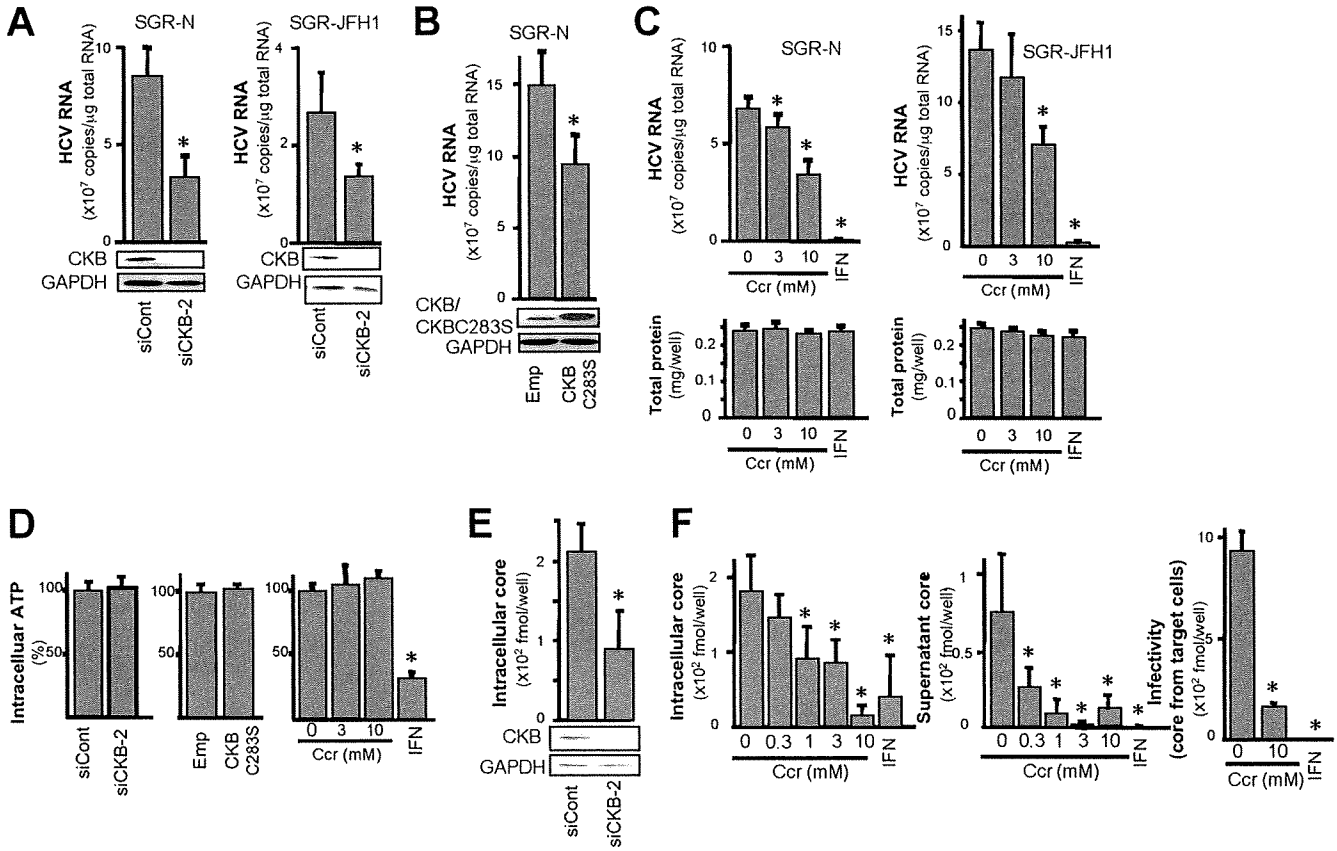

FIG. 2. Involvement of CKB in HCV replication. (A and E) Knockdown of endogenous CKB in SGR-N and SGR-JFH1 cells (A) or HCVcc-infected cells (E). Cells were transfected with siRNA against CKB (siCKB-2) or control siRNA (siCont) and were harvested at 72 h posttransfection. Real-time RT-PCR for HCV RNA levels and immunoblotting for CKB and GAPDH were performed. (B) SGR-N cells were transfected with pCAGCKB-C283S or empty vector, and HCV RNA levels and expression of CKB and CKB-C283S were determined 72 h posttransfection. SGR-N and SGR-JFH1 cells (C) or HCVcc-infected cells (F) were treated with Ccr at various concentrations for 72 h, followed by quantification of HCV RNAs and total cellular proteins. ATP levels (D) were determined after transfection with siCKB-2, pCAGCKB-C283S, or treatment with Ccr for 72 h in SGR-N cells. The ATP levels in the cells transfected with negative control siRNA (left), empty vector (middle), and no treatment (right) were set at 100%, respectively. (F) HCVcc-infected cells were treated with Ccr, and the viral core protein levels in cells (left) and supernatants (middle) were determined at 72 h postinfection. Collected culture supernatants were inoculated into naive Huh-7.5.1 cells after the removal of Ccr. After 72 h, the core proteins in cells were determined (right panel). All data are presented as averages and standard deviation values for at least triplicate samples. *, $P < 0.05$ against control such as transfection with siCont (A and E) or empty vector (B) or nontreatment (C, D, and F).

ported that interaction of CKB with some cellular proteins is required for local availability of CKB activity and local generation of ATP (22, 29). To examine the possible interaction of CKB with HCV NS proteins, HA-tagged CKB (HA-CKB) was coexpressed with FLAG-tagged NS proteins (NIHJ1 strain), followed by immunoprecipitation with an anti-FLAG antibody. CKB was shown to specifically interact with NS4A. No or little interaction was observed between CKB and either NS3, NS4B, NS5A, or NS5B (Fig. 3B). CKB-NS4A interaction was also found with the JFH-1 strain (Fig. 3C).

To identify the CKB region required for the interaction with NS4A, various deletion mutants of CKB were generated (Fig. 3A). An immunoprecipitation assay indicated that NS4A was coimmunoprecipitated with either a full-length CKB, a C-terminal deletion (aa 1 to 357), an N-terminal deletion (aa 297 to 381), or CKB-C283S, but not with aa 1 to 296, aa 1 to 247, or aa 1 to 184 (Fig. 3D, upper middle panel). Further, internal deletions of CKB (CKBdel297-357 and CKB-C283Sdel297-357) failed to interact with NS4A (Fig. 3D, lower panel), suggesting that aa 297 to 357 of CKB are important for its interaction with NS4A. It is noted that the expression of CKB aa 297 to 357 in cells was undetected, presumably due to its misfolding and/or instability. To verify a role for CKB-NS4A interaction in HCV RNA replication, we further determined the effect of expression of either CKB-C283S or its internal deletion lacking aa 297 to 357 (CKB-C283Sdel297-357) on viral replication in SGR-JFH1 cells. As expected, the HCV RNA level was significantly decreased by CKB-C283S, whereas this effect was not observed by CKB-C283Sdel297-357 (Fig. 3E).

NS4A is a 54-residue small protein composed of three domains: the N-terminal membrane anchor, the central domain responsible for interacting with NS3, and the C-terminal acidic domain. To define the portion in NS4A responsible for its interaction with CKB, we constructed three NS4A deletion mutants, each separately expressing one of the NS4A domains, with a FLAG tag (Fig. 3F). CKB proved to interact with the central domain, aa 21 to 39, of NS4A, which is involved in

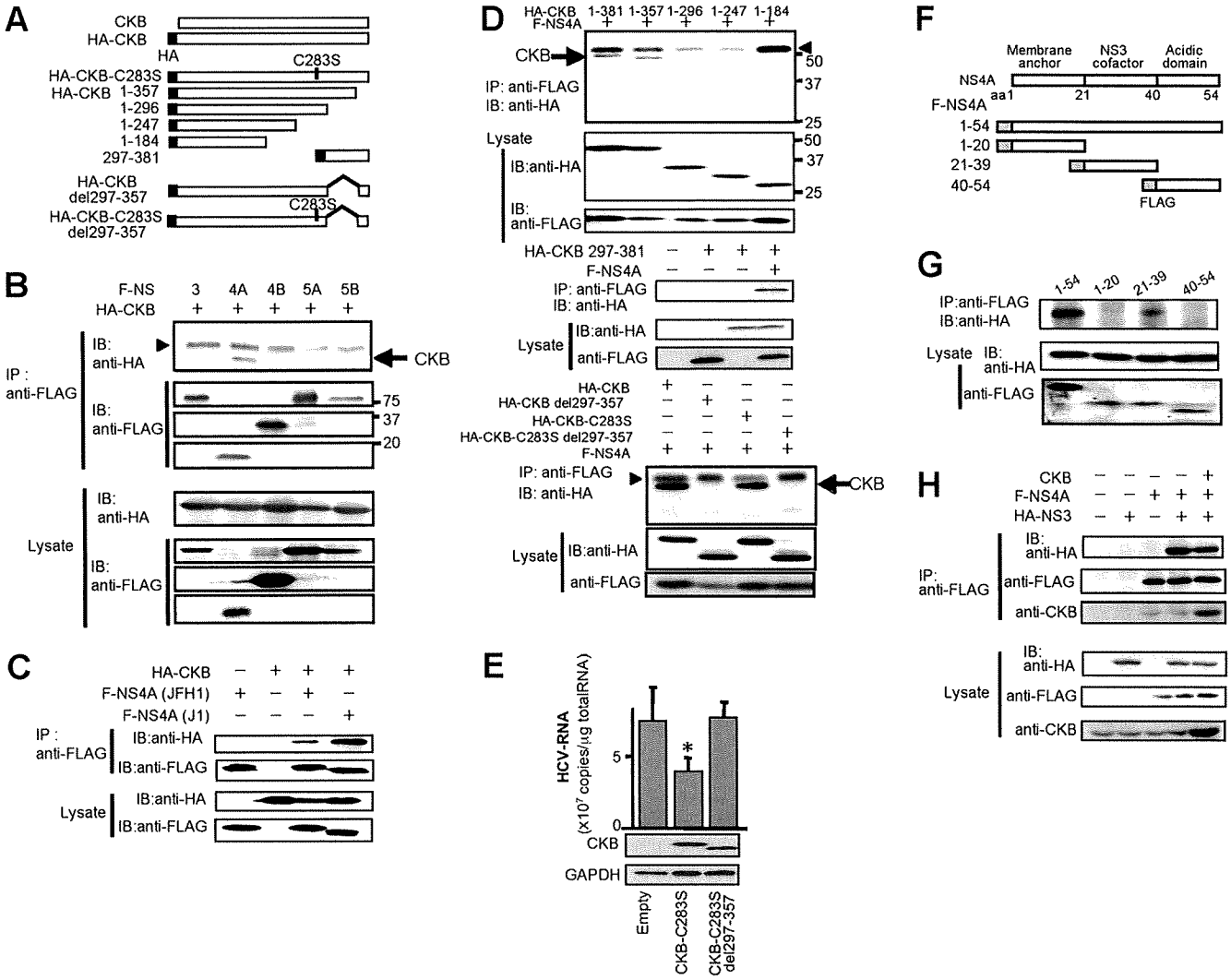

FIG. 3. CKB interacts with HCV NS4A. (A) Structures of CKB constructs used in the present study. A full-length wild-type CKB without an epitope tag (CKB) or with an N-terminal HA tag (HA-CKB), HA-CKB with deletions (aa 1 to 357, aa 1 to 296, aa 1 to 247, aa 1 to 184, and aa 297 to 381 and del297-357), CKB mutant at the catalytic site, Cys-283 (CKB-C283S) or CKB-C283S lacking aa 297 to 357 (CKB-C283Sdel297-357) are shown. HA-CKB was coexpressed with FLAG-tagged versions of each NS protein of strain NIHJ1 (B) or with NS4A of strain JFH-1 (C) in 293T cells and immunoprecipitated (IP) with an anti-FLAG antibody. Immunoprecipitates were subjected to immunoblotting (IB) with anti-HA or anti-FLAG antibody. (D) Each CKB deletion mutant was coexpressed with FLAG-NS4A in 293T cells. Immunoprecipitates were analyzed by immunoblotting. Arrow, CKB; arrowhead, immunoglobulin heavy chain. (E) SGR-JFH1 cells were transfected with the expression plasmid for CKB-C283S, CKB-C283Sdel297-357 or empty vector. At 72 h posttransfection, HCV RNA levels and the expression of CKB and CKB-C283S were determined by real-time RT-PCR and immunoblotting with anti-HA antibody, respectively. For HCV RNA quantitation, data are indicated as averages and standard deviations ($n = 3$). *, $P < 0.05$ against the empty vector control. (F) Structure of NS4A and NS4A constructs. FLAG-tagged NS4A (aa 1 to 54) or its truncated mutants (aa 1 to 20, aa 21 to 39, or aa 40 to 54) are shown. (G) Each NS4A deletion mutant was coexpressed with HA-CKB and analyzed as described above. (H) FLAG-NS4A was coexpressed with HA-NS3 or HA-NS3 and CKB, followed by immunoprecipitation with anti-FLAG antibody. Immunoprecipitates were analyzed by immunoblotting with anti-HA, anti-FLAG or anti-CKB antibody.

formation of the NS3-NS4A complex (Fig. 3G). We therefore investigate whether NS3-NS4A interaction is affected in the presence of CKB and found that exogenous expression of CKB has no influence on NS3-NS4A interaction, and a putative NS3-NS4A-CKB complex was detected in the coimmunoprecipitation analysis (Fig. 3H). Collectively, these results strongly suggest that CKB plays a key role in HCV RNA replication via interaction with NS4A.

Subcellular localization of CKB and NS4A in cells replicating HCV RNA. CKB is distributed throughout cells but is mainly localized in the perinuclear area (31), whereas NS4A is predominantly localized at the endoplasmic reticulum and mitochondrial membranes (37). We examined the possible subcellular colocalization of CKB and NS4A in SGR-N cells by immunofluorescence staining (Fig. 4A). CKB tended to gather in the perinuclear area of HCV replicating cells and was partially colocalized with NS4A in the area, sharing a dotlike structure. To further analyze the subcellular compartments in which CKB and NS4A coexist, we used double-labeling immunoelectron microscopy on SGR-N cells using antibodies against CKB and NS4A, with secondary antibodies coupled to 12- and 18-nm gold particles, respectively. One fraction of

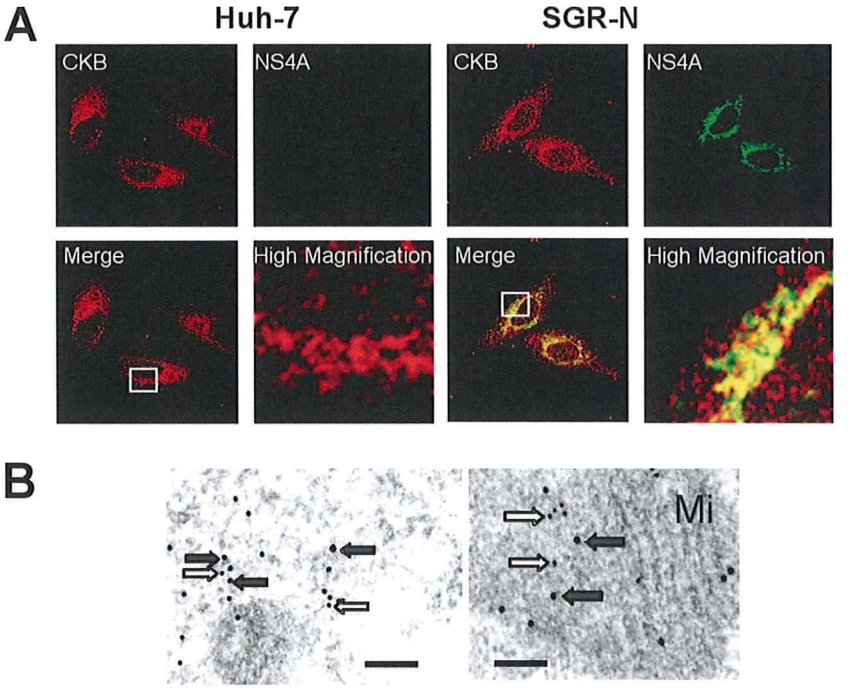

FIG. 4. Colocalization of CKB with HCV NS4A. (A) Indirect immunofluorescence analysis. The primary antibodies used were anti-CKB goat PAb (red) and anti-NS4A MAb (green). Merged images of red and green signals are shown. High-magnification panels are enlarged images of white squares in the merge panels. (B) Immunoelectron microscopic localization of CKB and NS4A. SGR-N cells were double-immunolabeled for CKB (12-nm gold particles; white arrows) and for NS4A (18-nm gold particle; gray arrows). Mi, mitochondria. Bars, 200 nm.

CKB colocalized with NS4A in the cytoplasmic electron-dense regions, presumably derived from altered or folded membrane structures (Fig. 4B, left panel) and mitochondria (Fig. 4B, right panel).

CKB enhances functional HCV replicase and NS3-4A helicase. NS4A is known to mediate membrane association of the NS3-4A complex and to function as a cofactor in NS3 enzyme activity. To understand the mechanism(s) underlying positive regulation of HCV RNA replication through CKB via its interaction with NS4A, we first investigated whether CKB modulates NS3-4A helicase activity. NS3-4A helicase is a member of the superfamily-2 DexH/D-box helicase, which unwinds RNA-RNA substrates in a 3′-to-5′ direction. During RNA replication, the NS3-4A helicase is believed to translocate along the nucleic acid substrate by changing its protein conformation, utilizing the energy of ATP hydrolysis (9). We then tested the effect of CKB on RNA- or DNA-unwinding activity using purified recombinant full-length NS3 and NS3-4A complex (12). As shown in Fig. 5A (left middle panel), both NS3 and NS3-4A helicase activity unwound dsRNA substrate most efficiently when CKB, ATP, and pCr were added to the reaction mixture. The enhancing effect of CKB was observed in the presence of pCr but not in the absence of it, suggesting that catalytic activity of CKB is important for its effect on the HCV helicase activity. Similar results were obtained from the DNA helicase assay using dsDNA substrate (Fig. 5B). To address the specificity of the stimulation by the CKB/pCr system, effects of PK and pPy, which are also involved in the ATP generation, were determined (Fig. 5A, right panels). Exogenous PK and pPy at the same concentrations as those of CKB and pCr used in the study exhibited no effect on the HCV helicase activity.

The effect of CKB on NS3-4A serine protease activity, which is considered to be ATP-independent, was also assessed in an in vitro protease assay using the purified viral proteins as mentioned above (Fig. 5C). As expected, NS3-4A complex exhibited significantly higher activity than NS3 alone; however, CKB did not affect the protease activities of NS3 or NS3-4A.

Finally, we investigated loss and gain of function of CKB in HCV replicase activity, which requires high-energy phosphate, in the context of semi-intact replicon cells. Miyanari et al. (33) reported that the function of the active HCV RC can be monitored in permeabilized replicon cells treated with digitonin. Thus, permeabilized replicon cells in the presence or absence of exogenous CKB were incubated with [α-^{32}P]UTP to detect newly synthesized RNA. As indicated in Fig. 5D, an ~8-kb band corresponding to HCV subgenomic RNA was most abundant in cells in the presence of exogenous CKB, ATP and pCr. The enhancing effect of CKB was observed in the presence but not in the absence of pCr, suggesting that catalytic activity of CKB is important for its effect on the replicase activity. As for the RNA helicase assay, exogenous PK and pPy did not enhance the replicase activity (data not shown). HCV replicase activity in permeabilized cells to which we had introduced siCKB-2 was diminished compared to that in siRNA control-treated cells. Interestingly, the replicase activity in the CKB-depleted cells was recovered by the addition of CKB. Thus, our findings suggest that CKB functions as a key regulator of HCV genome replication by controlling energy-dependent viral enzyme activities.

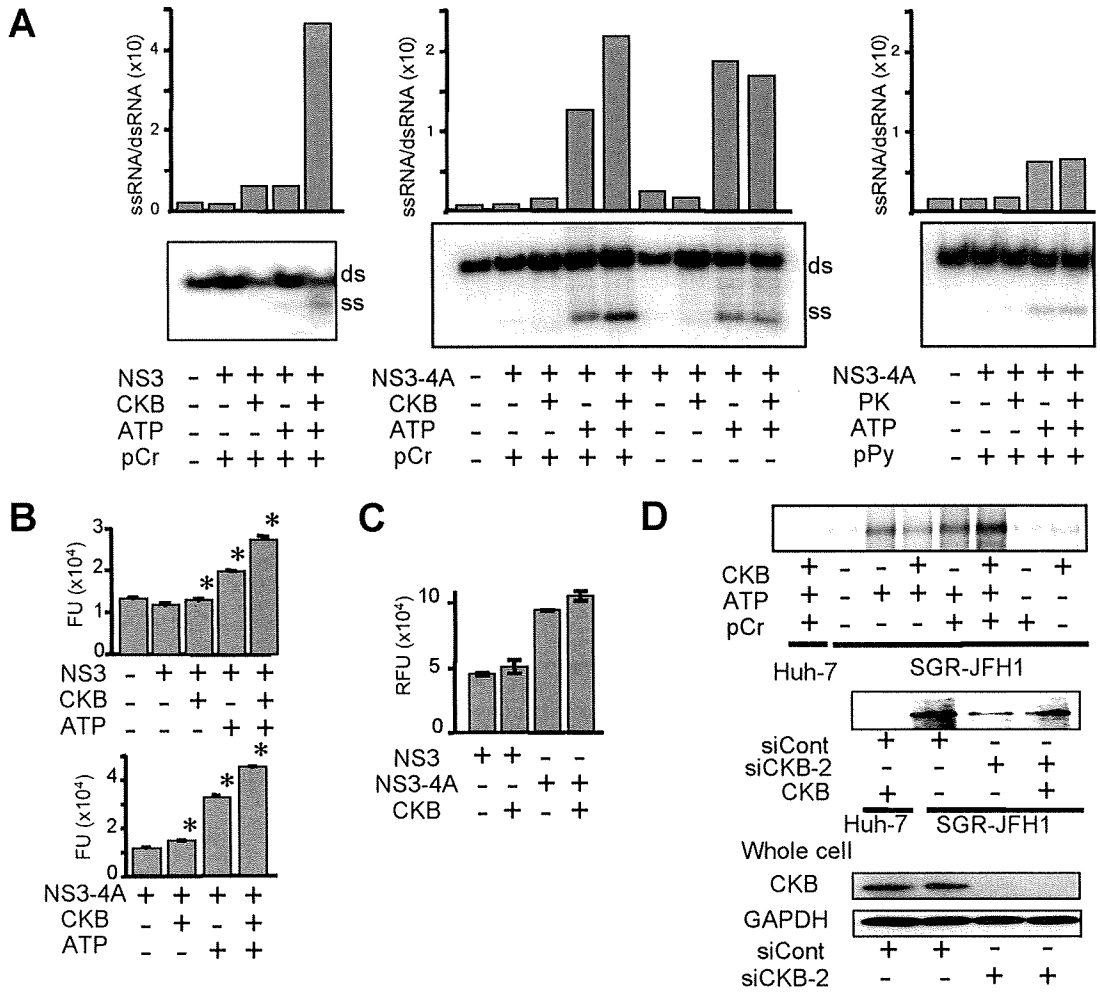

FIG. 5. CKB enhances NS3-4A helicase and HCV replicase activities. (A) In vitro RNA helicase activity of NS3-4A or NS3 was determined by detecting unwound single-strand RNA (ss) derived from the partially dsRNA substrate (ds). Band intensities corresponding to unwound products and those to dsRNA substrates were determined by ImageQuant 5.2 (Molecular Dynamics), and the ssRNA/dsRNA ratios were calculated. The results are representative of three similar experiments. (B) In vitro DNA helicase activity of NS3-4A or NS3 was analyzed by using a commercially available kit. The data represent averages and standard deviations ($n = 3$). *, $P < 0.05$ against the value without supplementation of CKB and ATP. (C) The in vitro HCV protease activity of NS3-4A or NS3 in the presence or absence of CKB was analyzed. Error bars represent standard deviations ($n = 3$). (D) Replicase activity in permeabilized replicon cells. The upper panel shows the activity for synthesis of HCV subgenomic RNA in the digitonin-permeabilized SGR-JFH1 cells with or without supplementation of CKB was measured. The middle panel shows results for SGR-JFH1 or Huh-7 cells that were transfected with siCKB-2 or siCont and permeabilized at 72 h posttransfection. The permeabilized cells with or without supplementation of CKB were subjected to the replicase assay. The lower panel shows the immunoblotting results for whole-cell lysates of siRNA-transfected cells.

DISCUSSION

Viral replication requires energy and macromolecule synthesis, and host cells provide the viruses with metabolic resources necessary for their efficient replication. Thus, it is highly likely that interaction of viruses with host cell metabolic pathways, including energy-generating systems, contributes to the virus growth cycle. In the regulation of HCV genome replication, the functions of the viral NS proteins that comprise the RC might be regulated by association in individual host cell factors. For example, hVAP-A and -B function as cofactors of modulating RC formation via interacting with NS5A and NS5B (13, 18). Cyclophilin B is involved in stimulating viral RNA binding activity via interacting with NS5B (49). FKBP8 (39) and hB-ind1 (45) play an important role in recruiting Hsp90 to RC via interacting with NS5A. However, the association of viral protein(s) with the cellular energy-generating system to directly regulate the activity of the RC has not been well understood.

In the present study, the accumulation of CKB, an ATP-generating enzyme, in the HCV RC-rich membrane fraction of viral replicating cells and its importance in replication of the HCV genome and production of infectious virions have been demonstrated. Enzymatic analyses with semi-intact replicon cells and purified NS3-4A protein revealed that CKB enhances the functional replicase and helicase of HCV. Its enhancing effect was observed in the presence of pCr but not in its absence, suggesting that the catalytic activity of CKB is important for enhancing the replicase and

helicase activities. Moreover, we clearly detected a CKB-NS4A complex using anti-tag antibodies in cotransfection experiments, but the endogenous complex could not be immunoprecipitated from cells expressing only endogenous levels of CKB, probably because of the inefficiency of the available antibodies. Further, a deletion of the NS4A-interacting region within an inactive mutant of CKB (CKB-C283S) resulted in the loss of its dominant-negative effect on HCV replication.

Creatine kinase, an evolutionarily conserved enzyme, is known to be critical for the maintenance and regulation of cellular energy stores in tissues with high and rapidly changing energy demands (48). In mammals, three cytosolic and two mitochondrial isoforms of CK, which share certain conserved regions, are expressed (35). The brain-type CK, CKB, plays a major role in cellular energy metabolism of nonmuscle cells, reversibly catalyzing the ATP-dependent phosphorylation of creatine and, hence, providing an ATP buffering system in subcellular compartments of high and fluctuating energy demand (21, 29). CKB is overexpressed in a wide range of tumor tissues and tumor cell lines, including hepatocellular carcinoma (32), and is used as a prognostic marker of cancer.

Although CK and creatine phosphate have been supplemented to in vitro replicase assays of some RNA viruses (15, 33), understanding of CKB function in the virus life cycle has been limited. One study indicated that the CK substrate analog, Ccr, exhibits antiviral activity against several herpesviruses but not influenza viruses or vesicular stomatitis virus (26). We have demonstrated here that HCV genome replication is downregulated by either treatment with Ccr, siRNA-mediated knockdown of CKB, or the exogenous expression of CKB-C283S. Coimmunoprecipitation experiments revealed that the essential domain within NS4A for the interaction with CKB is the NS4A central domain, aa 21 to 39, which is also responsible for NS3-4A complex formation. However, the NS3-4A interaction was not impaired by overexpression of CKB, and CKB was found to be able to form a complex with NS3-4A (Fig. 3H). Since CKB does not directly interact with NS3 (Fig. 3A), it is likely that NS3-4A-CKB association occurs through two interactions of NS3-4A and NS4A-CKB. We examined whether the formation of the ternary complex affects HCV enzymatic activities, possibly through conformational changes in the viral proteins, and found that CKB has no influence on NS3-4A protease activity (Fig. 5C). With regard to helicase activity, the effect of CKB on RNA unwinding activity by NS3-4A was similar to the effect of NS3 alone in the presence of ATP (Fig. 5A). It is conceivable that interaction with CKB causes no or little global change in the NS3-4A conformation and does not affect the viral helicase and protease activities.

In general, translation initiation in eukaryotes includes an ATP-dependent process such as unwinding the secondary structure in the 5′-untranslated region to permit assembly of 48S ribosomal complexes. It was reported, however, that 48S complex formation on the HCV internal ribosome entry site (IRES) has no requirement for ATP hydrolysis (25). In fact, we found that Huh-7 cells with or without gene silencing of CKB exhibited the same level of HCV IRES activity by transfection with IRES-reporter constructs (data not shown).

Collectively, we conclude that CKB is targeted to the HCV RC through its interaction with NS4A and functions as a positive regulator for the viral replicase by providing ATP. It is likely that the catalytic activity of CKB that associates with the viral RC is important for enhancing the RNA replication. The role of CKB-NS4A interaction in the enhancing effect seems to be limited. Although either knocking down CKB, expression of the dominant-negative mutant of CKB, or Ccr treatment resulted in the reduction of HCV replication (Fig. 2A to C), the total cellular ATP levels were not changed under these conditions (Fig. 2D). This suggests that CKB contributes to enhancing HCV replication through controlling the ATP level in the particular RC compartment. A tight coupling of a fast ATP regeneration and delivery system to the viral RC is advantageous for achieving efficient replication of the viral genome. To our knowledge, the findings presented here provide the first experimental evidence of the involvement of viral protein in recruiting an ATP generating/buffering system to the subcellular compartment for viral genome replication, a site with high-energy turnover. Given that the levels of HCV RNA were not dramatically diminished by the knocking down, dominant-negative mutant or Ccr, CKB may not be absolutely critical for the viral replication. One would argue that energy required for HCV genome replication can be partly complemented from the intracellular ATP pool.

Although there are several isoforms of CK as described above, the most abundant CK species expressed in Huh-7 cells in the present study was CKB, and no other isoenzymes, including mitochondrial CK, were detected by an isoform analysis based on the overlay gel technique (32; data not shown). Thus, the CKB isoenzyme appears to be a key molecule in the energy metabolism of HCV replicating cells. To identify potential HCV RC components, we used a comparative proteome analysis of the DRM fraction in cells harboring HCV subgenomic replicon and the DRM fractions in parental cells and then identified proteins that were more abundant in the fraction of HCV replicating cells. In agreement with similar previously reported approaches using the DRM or lipid raft fraction (30, 53), the functional categories of identified proteins included protein folding or assembly, cell metabolism and biosynthesis, cellular processes, and cytoskeleton organization (Table 1). Interestingly, Mannova et al. found that CKB was upregulated in the fraction of Huh-7 cells carrying the genotype 1b Con1 isolate-derived HCV replicon, as determined using stable isotope labeling by amino acids combined with one-dimensional electrophoresis (30). However, the effect of CKB on regulation of the HCV life cycle was not examined in that study.

In conclusion, CKB interacts with HCV NS4A and is important for efficient replication of the viral genome. Recruitment of CKB to the HCV replication machinery through its interaction with NS4A may have important implications for the maintenance or enhancement of the functional replicase activity in the RC compartment, where high-energy phosphoryl groups are required. A strategy for specific interception of energy supply at the subcellular site of HCV genome replication by disruption of the NS4A-CKB interface may lead to development of a new type of antiviral agent.

ACKNOWLEDGMENTS

We thank Francis V. Chisari (The Scripps Research Institute) for providing Huh-7.5.1 cells; Raffaele De Francesco (Istituto di Ricerche

di Biologia Molecolare, P. Angeletti) for providing purified recombinant NS3 and NS3-4A proteins; Oriental Yeast Co., Ltd., for providing human CKB cDNA; Minoru Fukuda (Laboratory for Electron Microscopy, Kyorin University School of Medicine) for electron microscopy; S. Yoshizaki, T. Shimoji, M. Kaga, M. Sasaki, and T. Date for technical assistance; and T. Mizoguchi for secretarial work.

This study was supported by a grant-in-aid for Scientific Research from the Japan Society for the Promotion of Science, from the Ministry of Health, Labor, and Welfare of Japan and from the Ministry of Education, Culture, Sports, Science, and Technology and by Research on Health Sciences focusing on Drug Innovation from the Japan Health Sciences Foundation, Japan, and by the Program for Promotion of Fundamental Studies in Health Sciences of the National Institute of Biomedical Innovation of Japan.

REFERENCES

1. **Aizaki, H., Y. Aoki, T. Harada, K. Ishii, T. Suzuki, S. Nagamori, G. Toda, Y. Matsuura, and T. Miyamura.** 1998. Full-length complementary DNA of hepatitis C virus genome from an infectious blood sample. Hepatology **27:** 621–627.
2. **Aizaki, H., K. J. Lee, V. M. Sung, H. Ishiko, and M. M. Lai.** 2004. Characterization of the hepatitis C virus RNA replication complex associated with lipid rafts. Virology **324:**450–461.
3. **Aizaki, H., K. Morikawa, M. Fukasawa, H. Hara, Y. Inoue, H. Tani, K. Saito, M. Nishijima, K. Hanada, Y. Matsuura, M. M. Lai, T. Miyamura, T. Wakita, and T. Suzuki.** 2008. Critical role of virion-associated cholesterol and sphingolipid in hepatitis C virus infection. J. Virol. **82:**5715–5724.
4. **Alter, H. J., and L. B. Seeff.** 2000. Recovery, persistence, and sequelae in hepatitis C virus infection: a perspective on long-term outcome. Semin. Liver Dis. **20:**17–35.
5. **Aoyagi, K., C. Ohue, K. Iida, T. Kimura, E. Tanaka, K. Kiyosawa, and S. Yagi.** 1999. Development of a simple and highly sensitive enzyme immunoassay for hepatitis C virus core antigen. J. Clin. Microbiol. **37:**1802–1808.
6. **Appel, N., T. Schaller, F. Penin, and R. Bartenschlager.** 2006. From structure to function: new insights into hepatitis C virus RNA replication. J. Biol. Chem. **281:**9833–9836.
7. **Bartenschlager, R., and V. Lohmann.** 2001. Novel cell culture systems for the hepatitis C virus. Antivir. Res. **52:**1–17.
8. **Brass, V., J. M. Berke, R. Montserret, H. E. Blum, F. Penin, and D. Moradpour.** 2008. Structural determinants for membrane association and dynamic organization of the hepatitis C virus NS3-4A complex. Proc. Natl. Acad. Sci. USA.
9. **Dumont, S., W. Cheng, V. Serebrov, R. K. Beran, I. Tinoco, Jr., A. M. Pyle, and C. Bustamante.** 2006. RNA translocation and unwinding mechanism of HCV NS3 helicase and its coordination by ATP. Nature **439:**105–108.
10. **Failla, C., L. Tomei, and R. De Francesco.** 1994. Both NS3 and NS4A are required for proteolytic processing of hepatitis C virus nonstructural proteins. J. Virol. **68:**3753–3760.
11. **Gallinari, P., D. Brennan, C. Nardi, M. Brunetti, L. Tomei, C. Steinkuhler, and R. De Francesco.** 1998. Multiple enzymatic activities associated with recombinant NS3 protein of hepatitis C virus. J. Virol. **72:**6758–6769.
12. **Gallinari, P., C. Paolini, D. Brennan, C. Nardi, C. Steinkuhler, and R. De Francesco.** 1999. Modulation of hepatitis C virus NS3 protease and helicase activities through the interaction with NS4A. Biochemistry **38:**5620–5632.
13. **Gao, L., H. Aizaki, J. W. He, and M. M. Lai.** 2004. Interactions between viral nonstructural proteins and host protein hVAP-33 mediate the formation of hepatitis C virus RNA replication complex on lipid raft. J. Virol. **78:**3480–3488.
14. **Gosert, R., D. Egger, V. Lohmann, R. Bartenschlager, H. E. Blum, K. Bienz, and D. Moradpour.** 2003. Identification of the hepatitis C virus RNA replication complex in Huh-7 cells harboring subgenomic replicons. J. Virol. **77:**5487–5492.
15. **Green, K. Y., A. Mory, M. H. Fogg, A. Weisberg, G. Belliot, M. Wagner, T. Mitra, E. Ehrenfeld, C. E. Cameron, and S. V. Sosnovtsev.** 2002. Isolation of enzymatically active replication complexes from feline calicivirus-infected cells. J. Virol. **76:**8582–8595.
16. **Guidotti, L. G., and F. V. Chisari.** 2006. Immunobiology and pathogenesis of viral hepatitis. Annu. Rev. Pathol. **1:**23–61.
17. **Guo, J. T., V. V. Bichko, and C. Seeger.** 2001. Effect of alpha interferon on the hepatitis C virus replicon. J. Virol. **75:**8516–8523.
18. **Hamamoto, I., Y. Nishimura, T. Okamoto, H. Aizaki, M. Liu, Y. Mori, T. Abe, T. Suzuki, M. M. Lai, T. Miyamura, K. Moriishi, and Y. Matsuura.** 2005. Human VAP-B is involved in hepatitis C virus replication through interaction with NS5A and NS5B. J. Virol. **79:**13473–13482.
19. **Hoofnagle, J. H.** 2002. Course and outcome of hepatitis C. Hepatology **36:**S21–S29.
20. **Ichimura, T., H. Yamamura, K. Sasamoto, Y. Tominaga, M. Taoka, K. Kakiuchi, T. Shinkawa, N. Takahashi, S. Shimada, and T. Isobe.** 2005. 14-3-3 proteins modulate the expression of epithelial Na+ channels by phosphorylation-dependent interaction with Nedd4-2 ubiquitin ligase. J. Biol. Chem. **280:**13187–13194.
21. **Inoue, K., S. Ueno, and A. Fukuda.** 2004. Interaction of neuron-specific K^+-Cl^- cotransporter, KCC2, with brain-type creatine kinase. FEBS Lett. **564:**131–135.
22. **Inoue, K., J. Yamada, S. Ueno, and A. Fukuda.** 2006. Brain-type creatine kinase activates neuron-specific K^+-Cl^- cotransporter KCC2. J. Neurochem. **96:**598–608.
23. **Kato, T., T. Date, M. Miyamoto, A. Furusaka, K. Tokushige, M. Mizokami, and T. Wakita.** 2003. Efficient replication of the genotype 2a hepatitis C virus subgenomic replicon. Gastroenterology **125:**1808–1817.
24. **Kato, T., A. Furusaka, M. Miyamoto, T. Date, K. Yasui, J. Hiramoto, K. Nagayama, T. Tanaka, and T. Wakita.** 2001. Sequence analysis of hepatitis C virus isolated from a fulminant hepatitis patient. J. Med. Virol. **64:**334–339.
25. **Lancaster, A. M., E. Jan, and P. Sarnow.** 2006. Initiation factor-independent translation mediated by the hepatitis C virus internal ribosome entry site. RNA **12:**894–902.
26. **Lillie, J. W., D. F. Smee, J. H. Huffman, L. J. Hansen, R. W. Sidwell, and R. Kaddurah-Daouk.** 1994. Cyclocreatine (1-carboxymethyl-2-iminoimidazolidine) inhibits the replication of human herpesviruses. Antivir. Res. **23:**203–218.
27. **Lindenbach, B. D., M. J. Evans, A. J. Syder, B. Wolk, T. L. Tellinghuisen, C. C. Liu, T. Maruyama, R. O. Hynes, D. R. Burton, J. A. McKeating, and C. M. Rice.** 2005. Complete replication of hepatitis C virus in cell culture. Science **309:**623–626.
28. **Lindenbach, B. D., B. M. Pragai, R. Montserret, R. K. Beran, A. M. Pyle, F. Penin, and C. M. Rice.** 2007. The C terminus of hepatitis C virus NS4A encodes an electrostatic switch that regulates NS5A hyperphosphorylation and viral replication. J. Virol. **81:**8905–8918.
29. **Mahajan, V. B., K. S. Pai, A. Lau, and D. D. Cunningham.** 2000. Creatine kinase, an ATP-generating enzyme, is required for thrombin receptor signaling to the cytoskeleton. Proc. Natl. Acad. Sci. USA **97:**12062–12067.
30. **Mannova, P., R. Fang, H. Wang, B. Deng, M. W. McIntosh, S. M. Hanash, and L. Beretta.** 2006. Modification of host lipid raft proteome upon hepatitis C virus replication. Mol. Cell Proteomics **5:**2319–2325.
31. **Manos, P., and J. Edmond.** 1992. Immunofluorescent analysis of creatine kinase in cultured astrocytes by conventional and confocal microscopy: a nuclear localization. J. Comp. Neurol. **326:**273–282.
32. **Meffert, G., F. N. Gellerich, R. Margreiter, and M. Wyss.** 2005. Elevated creatine kinase activity in primary hepatocellular carcinoma. BMC Gastroenterol. **5:**9.
33. **Miyanari, Y., M. Hijikata, M. Yamaji, M. Hosaka, H. Takahashi, and K. Shimotohno.** 2003. Hepatitis C virus nonstructural proteins in the probable membranous compartment function in viral genome replication. J. Biol. Chem. **278:**50301–50308.
34. **Moradpour, D., F. Penin, and C. M. Rice.** 2007. Replication of hepatitis C virus. Nat. Rev. Microbiol. **5:**453–463.
35. **Muhlebach, S. M., M. Gross, T. Wirz, T. Wallimann, J. C. Perriard, and M. Wyss.** 1994. Sequence homology and structure predictions of the creatine kinase isoenzymes. Mol. Cell Biochem. **133–134:**245–262.
36. **Murakami, K., K. Ishii, Y. Ishihara, S. Yoshizaki, K. Tanaka, Y. Gotoh, H. Aizaki, M. Kohara, H. Yoshioka, Y. Mori, N. Manabe, I. Shoji, T. Sata, R. Bartenschlager, Y. Matsuura, T. Miyamura, and T. Suzuki.** 2006. Production of infectious hepatitis C virus particles in three-dimensional cultures of the cell line carrying the genome-length dicistronic viral RNA of genotype 1b. Virology **351:**381–392.
37. **Nomura-Takigawa, Y., M. Nagano-Fujii, L. Deng, S. Kitazawa, S. Ishido, K. Sada, and H. Hotta.** 2006. Non-structural protein 4A of Hepatitis C virus accumulates on mitochondria and renders the cells prone to undergoing mitochondria-mediated apoptosis. J. Gen. Virol. **87:**1935–1945.
38. **Ohara-Imaizumi, M., T. Fujiwara, Y. Nakamichi, T. Okamura, Y. Akimoto, J. Kawai, S. Matsushima, H. Kawakami, T. Watanabe, K. Akagawa, and S. Nagamatsu.** 2007. Imaging analysis reveals mechanistic differences between first- and second-phase insulin exocytosis. J. Cell Biol. **177:**695–705.
39. **Okamoto, T., Y. Nishimura, T. Ichimura, K. Suzuki, T. Miyamura, T. Suzuki, K. Moriishi, and Y. Matsuura.** 2006. Hepatitis C virus RNA replication is regulated by FKBP8 and Hsp90. EMBO J. **25:**5015–5025.
40. **Oliver, I. T.** 1955. A spectrophotometric method for the determination of creatine phosphokinase and myokinase. Biochem. J. **61:**116–122.
41. **Shi, S. T., K. J. Lee, H. Aizaki, S. B. Hwang, and M. M. Lai.** 2003. Hepatitis C virus RNA replication occurs on a detergent-resistant membrane that cofractionates with caveolin-2. J. Virol. **77:**4160–4168.
42. **Shirakura, M., K. Murakami, T. Ichimura, R. Suzuki, T. Shimoji, K. Fukuda, K. Abe, S. Sato, M. Fukasawa, Y. Yamakawa, M. Nishijima, K. Moriishi, Y. Matsuura, T. Wakita, T. Suzuki, P. M. Howley, T. Miyamura, and I. Shoji.** 2007. E6AP ubiquitin ligase mediates ubiquitylation and degradation of hepatitis C virus core protein. J. Virol. **81:**1174–1185.
43. **Sunahara, Y., K. Uchida, T. Tanaka, H. Matsukawa, M. Inagaki, and Y. Matuo.** 2001. Production of recombinant human creatine kinase (r-hCK) isozymes by tandem repeat expression of M and B genes and characterization of r-hCK-MB. Clin. Chem. **47:**471–476.

44. **Suzuki, T., K. Ishii, H. Aizaki, and T. Wakita.** 2007. Hepatitis C viral life cycle. Adv. Drug Deliv. Rev. **59:**1200–1212.
45. **Taguwa, S., T. Okamoto, T. Abe, Y. Mori, T. Suzuki, K. Moriishi, and Y. Matsuura.** 2008. Human butyrate-induced transcript 1 interacts with hepatitis C virus NS5A and regulates viral replication. J. Virol. **82:**2631–2641.
46. **Takeuchi, T., A. Katsume, T. Tanaka, A. Abe, K. Inoue, K. Tsukiyama-Kohara, R. Kawaguchi, S. Tanaka, and M. Kohara.** 1999. Real-time detection system for quantification of hepatitis C virus genome. Gastroenterology **116:**636–642.
47. **Wakita, T., T. Pietschmann, T. Kato, T. Date, M. Miyamoto, Z. Zhao, K. Murthy, A. Habermann, H. G. Krausslich, M. Mizokami, R. Bartenschlager, and T. J. Liang.** 2005. Production of infectious hepatitis C virus in tissue culture from a cloned viral genome. Nat. Med. **11:**791–796.
48. **Wallimann, T., M. Wyss, D. Brdiczka, K. Nicolay, and H. M. Eppenberger.** 1992. Intracellular compartmentation, structure and function of creatine kinase isoenzymes in tissues with high and fluctuating energy demands: the 'phosphocreatine circuit' for cellular energy homeostasis. Biochem. J. **281**(Pt. 1):21–40.
49. **Watashi, K., N. Ishii, M. Hijikata, D. Inoue, T. Murata, Y. Miyanari, and K. Shimotohno.** 2005. Cyclophilin B is a functional regulator of hepatitis C virus RNA polymerase. Mol. Cell **19:**111–122.
50. **Wolk, B., D. Sansonno, H. G. Krausslich, F. Dammacco, C. M. Rice, H. E. Blum, and D. Moradpour.** 2000. Subcellular localization, stability, and trans-cleavage competence of the hepatitis C virus NS3-NS4A complex expressed in tetracycline-regulated cell lines. J. Virol. **74:**2293–2304.
51. **Wyss, M., and R. Kaddurah-Daouk.** 2000. Creatine and creatinine metabolism. Physiol. Rev. **80:**1107–1213.
52. **Yi, M., R. A. Villanueva, D. L. Thomas, T. Wakita, and S. M. Lemon.** 2006. Production of infectious genotype 1a hepatitis C virus (Hutchinson strain) in cultured human hepatoma cells. Proc. Natl. Acad. Sci. USA **103:**2310–2315.
53. **Yi, Z., C. Fang, T. Pan, J. Wang, P. Yang, and Z. Yuan.** 2006. Subproteomic study of hepatitis C virus replicon reveals Ras-GTPase-activating protein binding protein 1 as potential HCV RC component. Biochem. Biophys. Res. Commun. **350:**174–178.
54. **Zhong, J., P. Gastaminza, G. Cheng, S. Kapadia, T. Kato, D. R. Burton, S. F. Wieland, S. L. Uprichard, T. Wakita, and F. V. Chisari.** 2005. Robust hepatitis C virus infection in vitro. Proc. Natl. Acad. Sci. USA **102:**9294–9299.

JOURNAL OF VIROLOGY, Mar. 2009, p. 2389–2392 Vol. 83, No. 5
0022-538X/09/$08.00+0 doi:10.1128/JVI.01690-08

Proteasomal Turnover of Hepatitis C Virus Core Protein Is Regulated by Two Distinct Mechanisms: a Ubiquitin-Dependent Mechanism and a Ubiquitin-Independent but PA28γ-Dependent Mechanism▽

Ryosuke Suzuki,[1] Kohji Moriishi,[2] Kouichirou Fukuda,[1] Masayuki Shirakura,[1] Koji Ishii,[1] Ikuo Shoji,[3] Takaji Wakita,[1] Tatsuo Miyamura,[1] Yoshiharu Matsuura,[2] and Tetsuro Suzuki[1]*

Department of Virology II, National Institute of Infectious Diseases, Tokyo 162-8640,[1] Department of Molecular Virology, Research Institute for Microbial Diseases, Osaka University, Osaka 565-0871,[2] and Division of Microbiology, Kobe University Graduate School of Medicine, Hyogo 650-0017,[3] Japan

Received 8 August 2008/Accepted 5 December 2008

We have previously reported on the ubiquitylation and degradation of hepatitis C virus core protein. Here we demonstrate that proteasomal degradation of the core protein is mediated by two distinct mechanisms. One leads to polyubiquitylation, in which lysine residues in the N-terminal region are preferential ubiquitylation sites. The other is independent of the presence of ubiquitin. Gain- and loss-of-function analyses using lysineless mutants substantiate the hypothesis that the proteasome activator PA28γ, a binding partner of the core, is involved in the ubiquitin-independent degradation of the core protein. Our results suggest that turnover of this multifunctional viral protein can be tightly controlled via dual ubiquitin-dependent and -independent proteasomal pathways.

Hepatitis C virus (HCV) core protein, whose amino acid sequence is highly conserved among different HCV strains, not only is involved in the formation of the HCV virion but also has a number of regulatory functions, including modulation of signaling pathways, cellular and viral gene expression, cell transformation, apoptosis, and lipid metabolism (reviewed in references 9 and 15). We have previously reported that the E6AP E3 ubiquitin (Ub) ligase binds to the core protein and plays an important role in polyubiquitylation and proteasomal degradation of the core protein (22). Another study from our group identified the proteasome activator PA28γ/REG-γ as an HCV core-binding partner, demonstrating degradation of the core protein via a PA28γ-dependent pathway (16, 17). In this work, we further investigated the molecular mechanisms underlying proteasomal degradation of the core protein and found that in addition to regulation by the Ub-mediated pathway, the turnover of the core protein is also regulated by PA28γ in a Ub-independent manner.

Although ubiquitylation of substrates generally requires at least one Lys residue to serve as a Ub acceptor site (5), there is no consensus as to the specificity of the Lys targeted by Ub (4, 8). To determine the sites of Ub conjugation in the core protein, we used site-directed mutagenesis to replace individual Lys residues or clusters of Lys residues with Arg residues in the N-terminal 152 amino acids (aa) of the core (C152), within which is contained all seven Lys residues (Fig. 1A). Plasmids expressing a variety of mutated core proteins were generated by PCR and inserted into the pCAGGS (18). Each core-expressing construct was transfected into human embryonic kidney 293T cells along with the pMT107 (25) encoding a Ub moiety tagged with six His residues (His_6). Transfected cells were treated with the proteasome inhibitor MG132 for 14 h to maximize the level of Ub-conjugated core intermediates by blocking the proteasome pathway and were harvested 48 h posttransfection. His_6-tagged proteins were purified from the extracts by Ni^{2+}-chelation chromatography. Eluted protein and whole lysates of transfected cells before purification were analyzed by Western blotting using anticore antibodies (Fig. 1B). Mutations replacing one or two Lys residues with Arg in the core protein did not affect the efficiency of ubiquitylation: detection of multiple Ub-conjugated core intermediates was observed in the mutant core proteins comparable to the results seen with the wild-type core protein as previously reported (23). In contrast, a substitution of four N-terminal Lys residues (C152K6-23R) caused a significant reduction in ubiquitylation (Fig. 1B, lane 9). Multiple Ub-conjugated core intermediates were not detected in the Lys-less mutant (C152KR), in which all seven Lys residues were replaced with Arg (Fig. 1B, lane 11). These results suggest that there is not a particular Lys residue in the core protein to act as the Ub acceptor but that more than one Lys located in its N-terminal region can serve as the preferential ubiquitylation site. In rare cases, Ub is known to be conjugated to the N terminus of proteins; however, these results indicate that this does not occur within the core protein.

To investigate how polyubiquitylation correlates with proteasome degradation of the core protein, we performed kinetic analysis of the wild-type and mutated core proteins by use of the Ub protein reference (UPR) technique, which can compensate for data scatter of sample-to-sample variations such as levels of expression (10, 24). Fusion proteins expressed from UPR-based constructs (Fig. 2A) were cotranslationally cleaved by deubiquitylating enzymes, thereby generating equimolar quantities of the core proteins and the reference protein, dihydrofolate reductase-hemagglutinin (DHFR-HA) tag-modified Ub, in which the Lys at aa 48 was replaced by Arg to prevent its polyubiquitylation (Ub^{R48}). After 24 h of transfec-

* Corresponding author. Mailing address: Department of Virology II, National Institute of Infectious Diseases, 1-23-1 Toyama, Shinjuku-ku, Tokyo 162-8640, Japan. Phone: 81-3-5285-1111. Fax: 81-3-5285-1161. E-mail: tesuzuki@nih.go.jp.

▽ Published ahead of print on 17 December 2008.

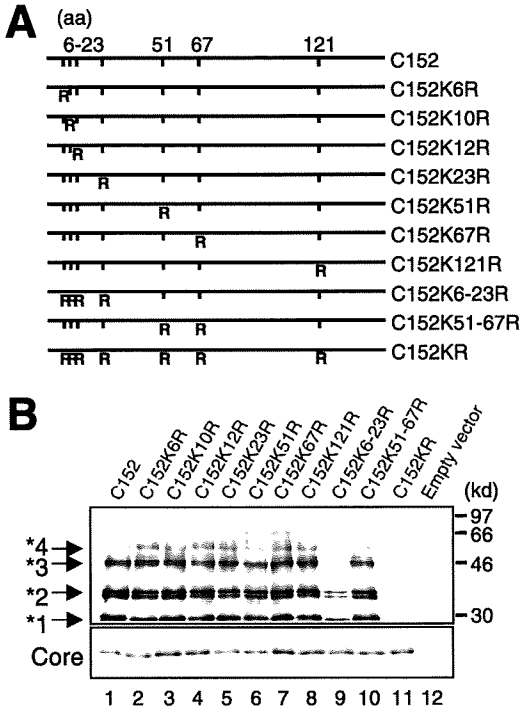

FIG. 1. In vivo ubiquitylation of HCV core protein. (A) The HCV core protein (N-terminal 152 aa) is represented on the top. The positions of the amino acid residues of the core protein are indicated above the bold lines. The positions of the seven Lys residues in the core are marked by vertical ticks. Substitution of Lys with Arg (R) is schematically depicted. (B) Detection of ubiquitylated forms of the core proteins. The transfected cells with core expression plasmids and pMT107 were treated with the proteasome inhibitor MG132 and harvested 48 h after transfection. His_6-tagged proteins were purified and subsequently analyzed by Western blot analysis using anticore antibody (upper panel). Core proteins conjugated to a number of His_6-Ub are denoted with asterisks. Whole lysates of transfected cells before purification were also analyzed (lower panel). Lanes 1 to 11, C152 to C152KR, as indicated for panel A. Lane 12; empty vector.

tion with UPR constructs, cells were treated with cycloheximide and the amounts of core proteins and DHFR-HA-Ub^{R48} at the indicated time points were determined by Western blot analysis using anticore and anti-HA antibodies. The mature form of the core protein, aa 1 to 173 (C173) (13, 20), and C152 were degraded with first-order kinetics (Fig. 2B and D). MG132 completely blocked the degradation of C173 and C152 (Fig. 2B), and C152K6-23R and C152KR were markedly stabilized (Fig. 2C). The half-lives of C173 and C152 were calculated to be 5 to 6 h, whereas those of C152K6-23R and C152KR were calculated to be 22 to 24 h (Fig. 2D), confirming that the Ub plays an important role in regulating degradation of the core protein. Nevertheless, these results also suggest possible involvement of the Ub-independent pathway in the turnover of the core protein, as C152KR is more destabilized than the reference protein (Fig. 2C and 2D).

We have shown that PA28γ specifically binds to the core protein and is involved in its degradation (16, 17). Recent studies demonstrated that PA28γ is responsible for Ub-independent degradation of the steroid receptor coactivator SRC-3 and cell cycle inhibitors such as p21 (3, 11, 12). Thus, we next investigated the possibility of PA28γ involvement in the degradation of either C152KR or C152. Since C152KR carries two amino acid substitutions in the PA28γ-binding region (aa 44 to 71) (17), we tested the influence of the mutations of C152KR on the interaction with PA28γ by use of a coimmunoprecipi-

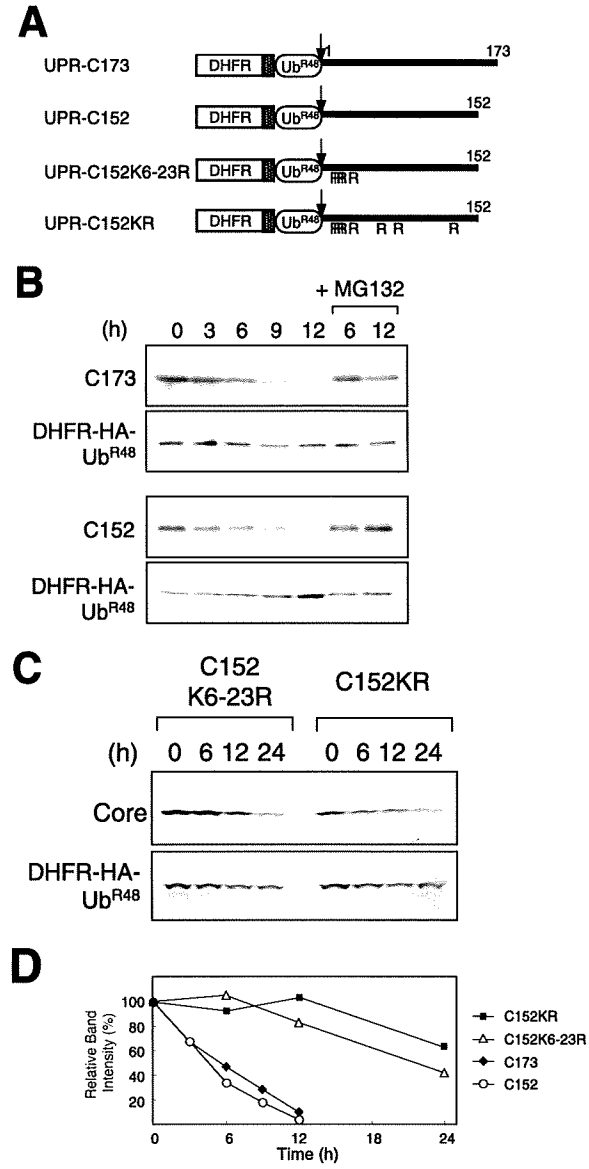

FIG. 2. Kinetic analysis of degradation of HCV core proteins. (A) The fusion constructs used in the UPR technique. Open boxes indicate the DHFR sequence, which is extended at the C terminus by a sequence containing the HA epitope (hatched boxes). Ub^{R48} moieties bearing the Lys-Arg substitution at aa 48 are represented by open ellipses. Bold lines indicate the regions of the core protein. The amino acid positions of the core protein are indicated above the bold lines. The arrows indicate the sites of in vivo cleavage by deubiquitylating enzymes. (B and C) Turnover of the core proteins. After a 24-h transfection with each UPR construct, cells were treated with 50 μg of cycloheximide/ml in the presence or absence of 10 μM MG132 for the different time periods indicated. Cells were lysed at the different time points indicated, followed by evaluation via sodium dodecyl sulfate-polyacrylamide gel electrophoresis and Western blot analysis using antibodies against the core protein and HA. (D) Quantitation of the data shown in panels B and C. At each time point, the ratio of band intensity of the core protein relative to the reference DHFR-HA-Ub^{R48} was determined by densitometry and is plotted as a percentage of the ratio at time zero.

tation assay. When Flag-tagged PA28γ (F-PA28γ) was expressed in cells along with C152 or C152KR, F-PA28γ precipitated along with both C152 and C152KR, indicating that PA28γ interacts with both core proteins (Fig. 3A). Figure 3B reveals the effect of exogenous expression of F-PA28γ on the steady-state levels of C152 and C152KR. Consistent with previous data (17), the expression level of C152 was decreased to a nearly undetectable level in the presence of PA28γ (Fig. 3B, lanes 1 and 3). Interestingly, exogenous expression of PA28γ led to a marked reduction in the amount of C152KR expressed (Fig. 3B, lanes 5 and 7). Treatment with MG132 increased the steady-state level of the C152KR in the presence of F-PA28γ as well as the level of C152 (Fig. 3B, lanes 4 and 8).

We further investigated whether PA28γ affects the turnover of Lys-less core protein through time course experiments. C152KR was rapidly destabilized and almost completely degraded in a 3-h chase experiment using cells overexpressing F-PA28γ (Fig. 3C, left panels). A similar result was obtained using an analogous Lys-less mutant of the full-length core protein C191KR (Fig. 3C, right panels), thus demonstrating that the Lys-less core protein undergoes proteasomal degradation in a PA28γ-dependent manner. These results suggest that PA28γ may play a role in accelerating the turnover of the HCV core protein that is independent of ubiquitylation.

Finally, we examined gain- and loss-of-function of PA28γ with respect to degradation of full-length wild-type (C191) and mutated (C191KR) core proteins in human hepatoma Huh-7 cells. As expected, exogenous expression of PA28γ or E6AP caused a decrease in the C191 steady-state levels (Fig. 4A). In contrast, the C191KR level was decreased with expression of PA28γ but not of E6AP. We further used RNA interference to inhibit expression of PA28γ or E6AP. An increase in the abundance of C191KR was observed with PA28γ small interfering RNA (siRNA) but not with E6AP siRNA (Fig. 4B). An increase in the C191 level caused by the activity of siRNA against PA28γ or E6AP was confirmed as well.

Taking these results together, we conclude that turnover of the core protein is regulated by both Ub-dependent and Ub-independent pathways and that PA28γ is possibly involved in Ub-independent proteasomal degradation of the core protein. PA28 is known to specifically bind and activate the 20S proteasome (19). Thus, PA28γ may function by facilitating the delivery of the core protein to the proteasome in a Ub-independent manner.

Accumulating evidence suggests the existence of proteasome-dependent but Ub-independent pathways for protein degradation, and several important molecules, such as p53, p73, Rb, SRC-3, and the hepatitis B virus X protein, have two distinct degradation pathways that function in a Ub-dependent and Ub-independent manner (1, 2, 6, 7, 14, 21, 27). Recently, critical roles for PA28γ in the Ub-independent pathway have been demonstrated; SRC-3 and p21 can be recognized by the 20S proteasome independently of ubiquitylation through their interaction with PA28γ (3, 11, 12). It has also been reported that phosphorylation-dependent ubiquitylation mediated by GSK3 and SCF is important for SRC-3 turnover (26). Nevertheless, the precise mechanisms underlying turnover of most of the proteasome substrates that are regulated in both Ub-dependent and Ub-independent manners are not well understood. To our knowledge, the HCV core protein is the first

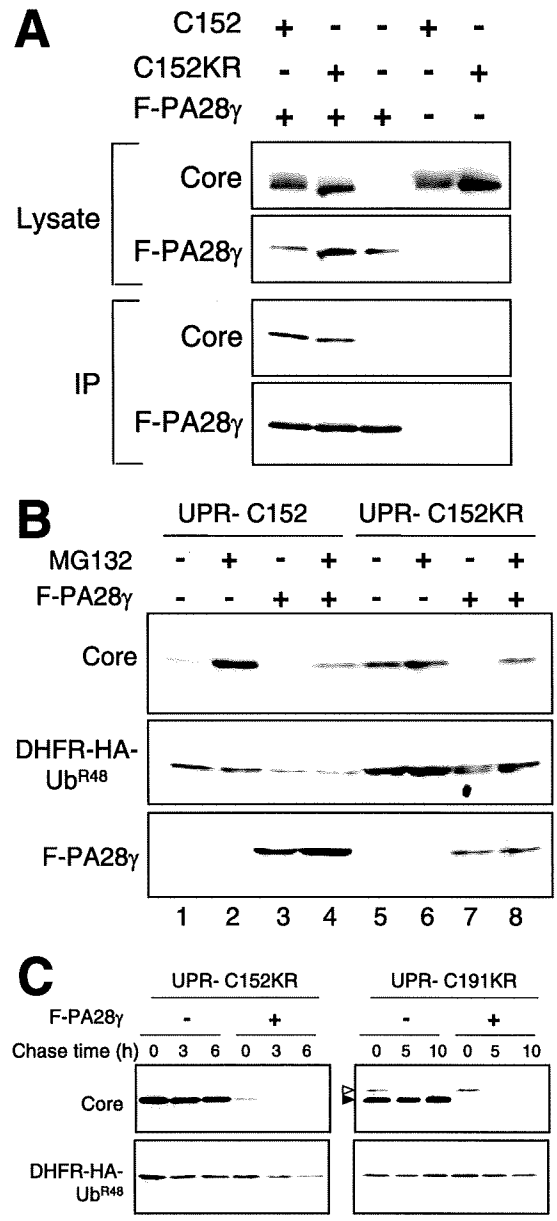

FIG. 3. PA28γ-dependent degradation of the core protein. (A) Interaction of the core protein with PA28γ. Cells were cotransfected with the wild-type (C152) or Lys-less (C152KR) core expression plasmid in the presence of a Flag-PA28γ (F-PA28γ) expression plasmid or an empty vector. The transfected cells were treated with MG132. After 48 h, the cell lysates were immunoprecipitated with anti-Flag antibody and visualized by Western blotting with anticore antibodies. Western blot analysis of whole cell lysates was also performed. (B) Degradation of the wild-type and Lys-less core proteins via the PA28γ-dependent pathway. Cells were transfected with the UPR construct with or without F-PA28γ. In some cases, cells were treated with 10 μM MG132 for 14 h before harvesting. Western blot analysis was performed using anticore, anti-HA, and anti-Flag antibodies. (C) After 24 h of transfection with UPR-C152KR and UPR-C191KR with or without F-PA28γ (an empty vector), cells were treated with 50 μg of cycloheximide/ml for different time periods as indicated (chase time). Western blot analysis was performed using anticore and anti-HA antibodies. The precursor core protein and the core that was processed, presumably by signal peptide peptidase, are denoted by open and closed triangles, respectively.

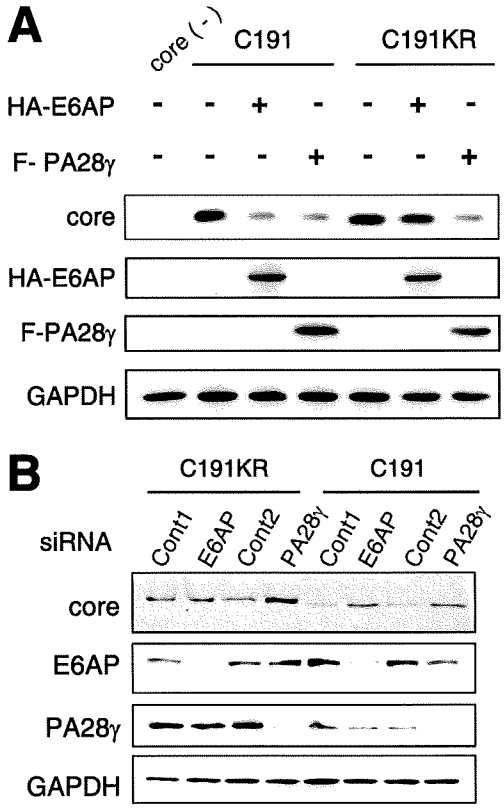

FIG. 4. Ub-dependent and Ub-independent degradation of the full-length core protein in hepatic cells. (A) Huh-7 cells were cotransfected with plasmids for the full-length core protein (C191) or its Lys-less mutant (C191KR) in the presence of F-PA28γ or HA-tagged-E6AP expression plasmid (HA-E6AP). After 48 h, cells were lysed and Western blot analysis was performed using anticore, anti-HA, anti-Flag, or anti-GAPDH. (B) Huh-7 cells were cotransfected with core expression plasmids along with siRNA against PA28γ or E6AP or with negative control siRNA. Cells were harvested 72 h after transfection and subjected to Western blot analysis.

viral protein studied that has led to identification of key cellular factors responsible for proteasomal degradation via dual distinct mechanisms. Although the question remains whether there is a physiological significance of the Ub-dependent and Ub-independent degradation of the core protein, it is reasonable to consider that tight control over cellular levels of the core protein, which is multifunctional and essential for viral replication, maturation, and pathogenesis, may play an important role in representing the potential for its functional activity.

This work was supported by a grant-in-aid for Scientific Research from the Japan Society for the Promotion of Science, from the Ministry of Health, Labor and Welfare of Japan, and from the Ministry of Education, Culture, Sports, Science and Technology, by Research on Health Sciences focusing on Drug Innovation from the Japan Health Sciences Foundation, Japan, and by the Program for Promotion of Fundamental Studies in Health Sciences of the National Institute of Biomedical Innovation of Japan.

REFERENCES

1. **Asher, G., J. Lotem, L. Sachs, C. Kahana, and Y. Shaul.** 2002. Mdm-2 and ubiquitin-independent p53 proteasomal degradation regulated by NQO1. Proc. Natl. Acad. Sci. USA **99:**13125–13130.
2. **Asher, G., P. Tsvetkov, C. Kahana, and Y. Shaul.** 2005. A mechanism of ubiquitin-independent proteasomal degradation of the tumor suppressors p53 and p73. Genes Dev. **19:**316–321.
3. **Chen, X., L. F. Barton, Y. Chi, B. E. Clurman, and J. M. Roberts.** 2007. Ubiquitin-independent degradation of cell-cycle inhibitors by the REGγ proteasome. Mol. Cell **26:**843–852.
4. **Ciechanover, A.** 1998. The ubiquitin-proteasome pathway: on protein death and cell life. EMBO J. **17:**7151–7160.
5. **Hershko, A., A. Ciechanover, and A. Varshavsky.** 2000. The ubiquitin system. Nat. Med. **6:**1073–1081.
6. **Jariel-Encontre, I., M. Pariat, F. Martin, S. Carillo, C. Salvat, and M. Piechaczyk.** 1995. Ubiquitinylation is not an absolute requirement for degradation of c-Jun protein by the 26 S proteasome. J. Biol. Chem. **270:**11623–11627.
7. **Jin, Y., H. Lee, S. X. Zeng, M. S. Dai, and H. Lu.** 2003. MDM2 promotes p21waf1/cip1 proteasomal turnover independently of ubiquitylation. EMBO J. **22:**6365–6377.
8. **Ju, D., and Y. Xie.** 2006. Identification of the preferential ubiquitination site and ubiquitin-dependent degradation signal of Rpn4. J. Biol. Chem. **281:**10657–10662.
9. **Lai, M. M. C., and C. F. Ware.** 1999. Hepatitis C virus core protein: possible roles in viral pathogenesis. Springer, Berlin, Germany.
10. **Lévy, F., N. Johnsson, T. Rumenapf, and A. Varshavsky.** 1996. Using ubiquitin to follow the metabolic fate of a protein. Proc. Natl. Acad. Sci. USA **93:**4907–4912.
11. **Li, X., L. Amazit, W. Long, D. M. Lonard, J. J. Monaco, and B. W. O'Malley.** 2007. Ubiquitin- and ATP-independent proteolytic turnover of p21 by the REGγ-proteasome pathway. Mol. Cell **26:**831–842.
12. **Li, X., D. M. Lonard, S. Y. Jung, A. Malovannaya, Q. Feng, J. Qin, S. Y. Tsai, M. J. Tsai, and B. W. O'Malley.** 2006. The SRC-3/AIB1 coactivator is degraded in a ubiquitin- and ATP-independent manner by the REGγ proteasome. Cell **124:**381–392.
13. **Liu, Q., C. Tackney, R. A. Bhat, A. M. Prince, and P. Zhang.** 1997. Regulated processing of hepatitis C virus core protein is linked to subcellular localization. J. Virol. **71:**657–662.
14. **Lonard, D. M., Z. Nawaz, C. L. Smith, and B. W. O'Malley.** 2000. The 26S proteasome is required for estrogen receptor-α and coactivator turnover and for efficient estrogen receptor-α transactivation. Mol. Cell **5:**939–948.
15. **Moradpour, D., F. Penin, and C. M. Rice.** 2007. Replication of hepatitis C virus. Nat. Rev. Microbiol. **5:**453–463.
16. **Moriishi, K., R. Mochizuki, K. Moriya, H. Miyamoto, Y. Mori, T. Abe, S. Murata, K. Tanaka, T. Miyamura, T. Suzuki, K. Koike, and Y. Matsuura.** 2007. Critical role of PA28γ in hepatitis C virus-associated steatogenesis and hepatocarcinogenesis. Proc. Natl. Acad. Sci. USA **104:**1661–1666.
17. **Moriishi, K., T. Okabayashi, K. Nakai, K. Moriya, K. Koike, S. Murata, T. Chiba, K. Tanaka, R. Suzuki, T. Suzuki, T. Miyamura, and Y. Matsuura.** 2003. Proteasome activator PA28γ-dependent nuclear retention and degradation of hepatitis C virus core protein. J. Virol. **77:**10237–10249.
18. **Niwa, H., K. Yamamura, and J. Miyazaki.** 1991. Efficient selection for high-expression transfectants with a novel eukaryotic vector. Gene **108:**193–199.
19. **Realini, C., C. C. Jensen, Z. Zhang, S. C. Johnston, J. R. Knowlton, C. P. Hill, and M. Rechsteiner.** 1997. Characterization of recombinant REGα, REGβ, and REGγ proteasome activators. J. Biol. Chem. **272:**25483–25492.
20. **Santolini, E., G. Migliaccio, and N. La Monica.** 1994. Biosynthesis and biochemical properties of the hepatitis C virus core protein. J. Virol. **68:**3631–3641.
21. **Sheaff, R. J., J. D. Singer, J. Swanger, M. Smitherman, J. M. Roberts, and B. E. Clurman.** 2000. Proteasomal turnover of p21Cip1 does not require p21Cip1 ubiquitination. Mol. Cell **5:**403–410.
22. **Shirakura, M., K. Murakami, T. Ichimura, R. Suzuki, T. Shimoji, K. Fukuda, K. Abe, S. Sato, M. Fukasawa, Y. Yamakawa, M. Nishijima, K. Moriishi, Y. Matsuura, T. Wakita, T. Suzuki, P. M. Howley, T. Miyamura, and I. Shoji.** 2007. E6AP ubiquitin ligase mediates ubiquitylation and degradation of hepatitis C virus core protein. J. Virol. **81:**1174–1185.
23. **Suzuki, R., K. Tamura, J. Li, K. Ishii, Y. Matsuura, T. Miyamura, and T. Suzuki.** 2001. Ubiquitin-mediated degradation of hepatitis C virus core protein is regulated by processing at its carboxyl terminus. Virology **280:**301–309.
24. **Suzuki, T., and A. Varshavsky.** 1999. Degradation signals in the lysine-asparagine sequence space. EMBO J. **18:**6017–6026.
25. **Treier, M., L. M. Staszewski, and D. Bohmann.** 1994. Ubiquitin-dependent c-Jun degradation in vivo is mediated by the δ domain. Cell **78:**787–798.
26. **Wu, R. C., Q. Feng, D. M. Lonard, and B. W. O'Malley.** 2007. SRC-3 coactivator functional lifetime is regulated by a phospho-dependent ubiquitin time clock. Cell **129:**1125–1140.
27. **Zhang, Z., and R. Zhang.** 2008. Proteasome activator PA28γ regulates p53 by enhancing its MDM2-mediated degradation. EMBO J. **27:**852–864.

ARTICLE
Journal of Cellular Biochemistry 106:1123–1135 (2009)

Identification of Annexin A1 as a Novel Substrate for E6AP-Mediated Ubiquitylation

Tetsu Shimoji,[1] Kyoko Murakami,[1] Yuichi Sugiyama,[1] Mami Matsuda,[1] Sachiko Inubushi,[2] Junichi Nasu,[1] Masayuki Shirakura,[1] Tetsuro Suzuki,[1] Takaji Wakita,[1] Tatsuya Kishino,[3] Hak Hotta,[2] Tatsuo Miyamura,[1] and Ikuo Shoji[1,2*]

[1]*Department of Virology II, National Institute of Infectious Diseases, Shinjuku-ku, Tokyo, Japan*
[2]*Division of Microbiology, Kobe University Graduate School of Medicine, Kobe, Hyogo, Japan*
[3]*Division of Functional Genomics, Center for Frontier Life Sciences, Nagasaki University, Nagasaki, Japan*

ABSTRACT

E6-associated protein (E6AP) is a cellular ubiquitin protein ligase that mediates ubiquitylation and degradation of p53 in conjunction with the high-risk human papillomavirus E6 proteins. However, the physiological functions of E6AP are poorly understood. To identify a novel biological function of E6AP, we screened for binding partners of E6AP using GST pull-down and mass spectrometry. Here we identified annexin A1, a member of the annexin superfamily, as an E6AP-binding protein. Ectopic expression of E6AP enhanced the degradation of annexin A1 in vivo. RNAi-mediated downregulation of endogenous E6AP increased the levels of endogenous annexin A1 protein. E6AP interacted with annexin A1 and induced its ubiquitylation in a Ca^{2+}-dependent manner. GST pull-down assay revealed that the annexin repeat domain III of annexin A1 is important for the E6AP binding. Taken together, our data suggest that annexin A1 is a novel substrate for E6AP-mediated ubiquitylation. Our findings raise the possibility that E6AP may play a role in controlling the diverse functions of annexin A1 through the ubiquitin-proteasome pathway. J. Cell. Biochem. 106: 1123–1135, 2009.

KEY WORDS: E6AP; ANNEXIN A1; UBIQUITIN; DEGRADATION

The ubiquitin/26S proteasome pathway plays important roles in the control of many basic cellular processes, such as cell cycle progression, signal transduction, transcriptional regulation, DNA repair, and the regulation of inflammation responses [Hershko and Ciechanover, 1998]. Ubiquitin is a 76-aa polypeptide that is highly conserved among eukaryotic organisms. The ubiquitin-proteasome pathway consists of an enzymatic cascade that ubiquitylates proteins, thereby targeting them for proteasomal degradation. The E1 ubiquitin-activating enzyme binds ubiquitin through a thioester linkage in an ATP-dependent manner [Ciechanover et al., 1981; Haas and Rose, 1982]. The activated ubiquitin is then transferred to the E2 ubiquitin-conjugating enzyme. E2 works in conjunction with the E3 ubiquitin-protein ligase, which is responsible for conferring substrate specificity [Hershko et al., 1986]. E3 mediates the transfer of ubiquitin to the target protein. The polyubiquitylated substrates are rapidly recognized and degraded by the 26S proteasome [Ciechanover, 1998; Ciechanover et al., 2000].

E6-associated protein (E6AP) was initially identified as the cellular factor that stimulates ubiquitin-dependent degradation of the tumor suppressor p53 in conjunction with the E6 protein of cervical cancer-associated human papillomavirus (HPV) types 16 and 18 [Huibregtse et al., 1993a; Scheffner et al., 1994]. The E6–E6AP complex functions as an E3 ubiquitin ligase in the ubiquitylation of p53 [Scheffner et al., 1993]. E6AP is the prototype of a family of ubiquitin ligases called HECT domain ubiquitin ligases, all of which contain a domain *h*omologous to the

Abbreviations used: E6AP, E6-associated protein; HPV, human papillomavirus; MALDI-TOF, matrix assisted laser desorption ionization-time of flight; MS, mass spectrometry; HCV, hepatitis C virus; MAb, monoclonal antibody; PAb, polyclonal antibody; GAPDH, glyceraldehydes-3-phosphate dehydrogenase; CHX, cycloheximide.

T. Shimoji and K. Murakami contributed equally to this work.

Grant sponsor: Japan Health Sciences Foundation; Grant sponsor: Ministry of Health, Labor, and Welfare; Grant sponsor: Promotion of Fundamental Studies in Health Sciences of the National Institute of Biomedical Innovation (NIBIO), Japan.

*Correspondence to: Ikuo Shoji, MD, PhD, Division of Microbiology, Kobe University Graduate School of Medicine, 7-5-1 Kusunoki-cho, Chuo-ku, Kobe, Hyogo 650-0017, Japan. E-mail: ishoji@med.kobe-u.ac.jp

Received 26 November 2008; Accepted 14 January 2009 • DOI 10.1002/jcb.22096 • 2009 Wiley-Liss, Inc.
Published online 9 February 2009 in Wiley InterScience (www.interscience.wiley.com).

*E*6AP carboxyl *t*erminus [Huibregtse et al., 1995]. Known substrates of the E6–E6AP complex include the tumor suppressor p53 [Scheffner et al., 1993], the PDZ domain-containing protein scribble [Nakagawa and Huibregtse, 2000] and NFX1-91, a transcriptional repressor of the gene encoding hTERT [Gewin et al., 2004]. Interestingly, E6AP is not involved in the ubiquitylation of p53 in the absence of E6 [Talis et al., 1998]. Several potential E6-independent substrates for E6AP have been identified, such as HHR23A and HHR23B (the human orthologs of *Saccharomyces cerevisae* Rad23) [Kumar et al., 1999], Blk (a member of the Src family kinases) [Oda et al., 1999], Mcm7 (which is involved in DNA replication) [Kuhne and Banks, 1998], trihydrophobin 1 [Yang et al., 2007], and AIB1 (a steroid receptor coactivator) [Mani et al., 2006].

Some patients with Angelman syndrome, a severe neurological disorder linked to E6AP, have mutations within the catalytic cleft that have been shown to reduce E6AP ubiquitin ligase activity [Kishino et al., 1997; Cooper et al., 2004]. Despite the significant progress in the study of Angelman syndrome-associated E6AP mutations, none of the identified E6AP substrates have been directly linked to the disorder. The physiological functions of E6AP are poorly understood at present.

In an attempt to identify novel substrates of E6AP, we identified annexin A1 (formerly known as lipocortin 1) as an E6AP-binding protein. Annexin A1 is a 37-kDa member of the annexin superfamily of Ca^{2+} and phospholipid-binding proteins [Lim and Pervaiz, 2007]. Annexin A1 is involved in the inhibition of cell proliferation, anti-inflammatory effects, and the regulation of cell differentiation. In addition, annexin A1 is involved in the regulation of cell death signaling, phagocytosis of apoptosis, and the process of carcinogenesis [Buckingham et al., 2006; Lim and Pervaiz, 2007]. Annexin A1 is phosphorylated by various kinases such as tyrosine kinase, pp60c-src [Varticovski et al., 1988], protein kinase C [Oudinet et al., 1993], epidermal growth factor receptor protein kinase [Haigler et al., 1987], and hepatocyte growth factor receptor kinase [Skouteris and Schroder, 1996].

In this study, we have examined the possibility that the stability of annexin A1 is regulated through E6AP-dependent ubiquitylation. Our study revealed that E6AP mediates ubiquitin-dependent degradation of annexin A1 in a Ca^{2+}-dependent manner. Our results raise the possibility that E6AP may have a role in controlling the diverse functions of annexin A1.

MATERIALS AND METHODS

CELL CULTURE AND TRANSFECTION

Human embryonic kidney (HEK) 293T cells, and human cervical carcinoma C33-A cells were cultured in Dulbecco's modified Eagle's medium (DMEM) (Sigma, St. Louis, MO) supplemented with 50 IU/ml penicillin, 50 μg/ml streptomycin (Invitrogen, Carlsbad, CA), and 10% (v/v) fetal bovine serum (FBS) (JRH Biosciences, Lenexa, KS) at 37°C in a 5% CO_2 incubator. HEK 293T cells and C33-A cells were transfected with plasmid DNA using FuGene 6 transfection reagents (Roche, Mannheim, Germany). The *Spodoptera frugiperda* (Sf) 9 cells were cultured in TC100 (JRH Biosciences) supplemented with 10% (v/v) FBS and 100 μg/ml kanamycin at 26°C in an incubator. The *Trichoplusia ni* (Tn) 5 cells were cultured in Ex-Cell 405 (JRH Biosciences) at 26°C in an incubator.

PLASMIDS AND RECOMBINANT BACULOVIRUSES

To express annexin A1 as a FLAG-tagged fusion protein in mammalian cells, annexin A1 fragment was amplified from pKK-trc-lipo-155 (a kind gift from Dr. Browning, Biogen) by polymerase chain reaction (PCR) using two oligonucleotides, 5′-TATCCCGG-GAACCACCATGGCAATGGTATCAGAATTCC-3′ and 5′-TATGCGG-CCGCTTACTTATCGTCGTCATCCTTGTAATCGTTTCCTCCACAAAG-AGCC-3′. The FLAG-tag sequence was fused to the C-terminus of the annexin A1 gene in frame. The amplified PCR fragment was digested with *Sma*I and *Not*I, purified, and subcloned into pCAGGS [Niwa et al., 1991], resulting in pCAG-annexin A1-FLAG. To express E6AP and the active-site cysteine-to-alanine mutant of E6AP in mammalian cells, pCAG-HA-E6AP isoform II and pCAG-HA-E6AP C-A were used [Shirakura et al., 2007]. The C-A mutation was introduced at the site of E6AP C843 [Kao et al., 2000]. To express Nedd4, pCAG-HA-Nedd4 was constructed. To make a fusion protein consisting of glutathione S-transferase (GST) fused to the N-terminus of E6AP in *Escherichia coli* (*E. coli*), pGEX-E6AP was used [Shirakura et al., 2007]. Recombinant baculoviruses expressing GST-E6AP were described previously [Shirakura et al., 2007]. To express hexahistidine (His)-tagged annexin A1 in *E. coli*, annexin A1 fragment was amplified from pKK-trc-lipo-155 by PCR using two oligonucleotides, 5′-TATCCCGGGAACCACCATGGCAATGG-TATCAGAATTCC-3′ and 5′-ATAGCGGCCGCGTTTCCTCCACAAA-GAGCC-3′. The PCR fragment was purified and digested with *Sma*I and *Not*I. pET21b was digested with *Nde*I, blunt ended with a DNA blunting kit (Takara, Japan), and digested with *Not*I. Then, the PCR fragment of annexin A1 was ligated into the pET21b fragment, resulting in pET21b-annexin A1. To map the E6AP-binding site on annexin A1 protein, a series of expression plasmids for GST-annexin A1 fusion proteins were constructed by amplifying annexin A1 gene fragments with PCR using sense primers containing *Sma*I site and antisense primers containing a *Not*I site. The amplified PCR fragments were subcloned into pGEM T-Easy (Promega, Madison, WI) and verified by sequencing. Then, the annexin A1 gene fragments were digested with *Sma*I and *Not*I and ligated into the *Sma*I–*Not*I site of pGEX 4T-1 (GE Healthcare, Uppsala, Sweden). The annexin A1 (1-41) gene fragment was amplified from pET21b-annexin A1 by PCR using two oligonucleotides, 5′-TATCCCGG-GAACCACCATGGCAATGGTATCAGAATTCC-3′ and 5′-ATATAGC-GGCCGCTTAGGTAGGATAGGGGCTCACCGCT-3′. The PCR primers used to amplify the annexin A1 fragments were as follows:

Annexin A1 (42–346): 5′-TATCCCGGGAACCACCATGTTCAAT-CCATCCTCGGATGTCG-3′ and 5′-ATATAGCGGCCGCTTAGTTT-CCTCCACAAAGAGCC-3′.
Annexin A1 (42–113): 5′-AAACCCGGGTATGTTCAATCCATCCT-CGGATGTCG-3′ and 5′-TTTGCGGCCGCTTATTTTAGCAGAGC-TAAAACAAC-3′.
Annexin A1 (114–195): 5′-AAACCCGGGTATGACTCCAGCG-CAATTTGATGC-3′ and 5′-TTTGCGGCCGCTTAATTCACACCAA-AGTCCTCAG-3′.

Annexin A1 (196–274): 5′-AAACCCGGGTATGGAAGACTTGG-CTGATTCAG-3′ and 5′-TTTGCGGCCGCTTAGCTTGTGGCGCAC-TTCACG-3′.
Annexin A1 (275–346): 5′-AAACCCGGGTATGAAACCAGCTTT-CTTTGCAGAG-3′ and 5′-ATATAGCGGCCGCTTAGTTTCCTCCA-CAAAGAGCC-3′.
Annexin A1 (42–195): 5′-AAACCCGGGTATGTTCAATCCATCC-TCGGATGTCG-3′ and 5′-TTTGCGGCCGCTTAATTCACACCAAA-GTCCTCAG-3′.
Annexin A1 (114–274): 5′-AAACCCGGGTATGACTCCAGCGCA-ATTTGATGC-3′ and 5′-TTTGCGGCCGCTTAGCTTGTGGCGCAC-TTCACG-3′.
Annexin A1 (196–346): 5′-AAACCCGGGTATGGAAGACTTGG-CTGATTCAG-3′ and 5′-ATATAGCGGCCGCTTAGTTTCCTCCAC-AAAGAGCC-3′.

The sequences of the inserts were extensively verified using an ABI PRISM 3100-Avant Genetic Analyzer (Applied Biosystems, Foster City, CA). To express GST, GST-E6AP, and MEF-E6AP in the baculovirus expression system, recombinant baculoviruses were recovered using a BaculoGold transfection kit (Pharmingen, San Diego, CA) as described previously [Shirakura et al., 2007].

ANTIBODIES

The mouse monoclonal antibodies (MAbs) used in this study were anti-HA MAb (12CA5) (Roche), anti-HA 16B12 MAb (HA.11; BabCO), anti-Annexin I MAb (BD Biosciences, San Jose, CA), anti-glyceraldehyde-3-phosphate dehydrogenase (GAPDH) MAb (Chemicon, Temecula, CA), anti-GST MAb (Santa Cruz Biotechnology, Santa Cruz, CA), anti-ubiquitin MAb (Chemicon), anti-E6AP MAb (E6AP-330) (Sigma), and anti-β-actin MAb (Ab-1) (Calbiochem, San Diego, CA). The polyclonal antibodies (PAbs) used in this study were anti-HA rabbit PAb (Y-11; Santa Cruz Biotechnology), anti-FLAG rabbit PAb (F7425; Sigma), anti-E6AP rabbit PAb (H-182; Santa Cruz Biotechnology), and anti-GST goat PAb (Amersham Bioscience, Buckinghamshire, UK).

IDENTIFICATION OF E6AP-BINDING PROTEINS WITH MALDI-TOF MASS SPECTROMETRY

To screen for potential E6AP-binding proteins, GST pull-down assays were performed using GST-E6AP and ten 225 cm^2-flasks (Corning, New York, NY) of confluent C-33A cells as the source of protein. The cells were lysed in 15 ml of the cell lysis buffer (100 mM Tris–HCl, pH 7.4, 100 mM NaCl, 0.5% Triton X-100 [ICE Biomedicals, Aurora, OH], Complete protease inhibitor cocktail [Roche]). The samples were incubated at 4°C for 1 h, and centrifuged at 13,000*g* for 30 min. The supernatants were collected and pre-cleared with 250 μl of 50% slurry glutathione-Sepharose 4B beads (Amersham Bioscience) to remove proteins that can nonspecifically bind to glutathione-Sepharose 4B beads. The supernatants were then pre-cleared with 250 μg of GST immobilized on glutathione-Sepharose 4B beads to remove proteins which can bind to GST. Then, the supernatant was collected, mixed with 250 μg of GST-E6AP or GST immobilized on glutathione-Sepharose 4B beads, and incubated for 1 h at 4°C. The beads were collected and washed with the cell lysis buffer three times. To remove the bound proteins from GST-E6AP, the bound proteins were released with the releasing buffer (10 mM Tris–HCl, pH 7.4, 150 mM NaCl, 1% sodium deoxycholate, 0.1% sodium dodecyl sulfate [SDS], 1% Triton X-100) five times. The released proteins were mixed with 20% (w/v) trichloroacetic acid (TCA) and incubated at 4°C for 30 min. After centrifugation, the TCA-precipitated samples were washed with ice-cold acetone four times, dried, and lysed in SDS-polyacrylamide gel electrophoresis (SDS–PAGE) loading buffer. The samples were separated by 7.5% SDS–PAGE and stained with Coomassie brilliant blue (CBB). The specific protein bands were excised from the gel and subjected to in-gel trypsin digestion. The tryptic peptide mixtures were analyzed by MALDI-TOF/MS analysis [Kaji et al., 2000]. Prior to MALDI-TOF/MS analysis, the peptide mixtures were desalted using C18 Zip Tips (Millipore, Bedford, MA) according to the manufacturer's instructions. The peptide data were collected in the reflection mode and with positive polarity, using a saturated solution of α-cyano-4-hydroxycinnamic acid (Sigma) in 50% acetonitrile (PE Biosystems, Foster City, CA) and 0.1% trifluoroacetic acid as the matrix. Spectra were obtained using a Voyger DE-STR MALDI-TOF mass spectrometer (PE Biosystems). The database-fitting program MS-Fit at the website (http://jpsl.ludwig.edu.au/ucsfhtml3.4/msfit.htm) of the University of California, San Francisco was used to interpret the MS spectra of the protein digests.

EXPRESSION AND PURIFICATION OF RECOMBINANT PROTEINS

E. coli BL21 (DE3) cells were transformed with plasmids expressing GST fusion protein or His-tagged protein and grown at 37°C. Expression of the fusion protein was induced by 1 mM isopropyl-β-D-thiogalactopyranoside at 25°C for 4 h. Bacteria were harvested, suspended in lysis buffer (phosphate-buffered saline [PBS] containing 1% Triton X-100, Complete protease inhibitor cocktail, EDTA free [Roche]), and sonicated on ice.

Hi5 cells were infected with the recombinant baculoviruses to produce GST-E6AP or GST. GST-E6AP and GST-fusion proteins were purified on glutathione-Sepharose beads (Amersham Bioscience) according to the manufacturer's protocols. His-tagged proteins were purified on Ni-NTA beads (Qiagen, Hilden, Germany) according to the manufacturer's protocols. MEF-E6AP and MEF-E6AP C-A [Shirakura et al., 2007] were purified on anti-FLAG M2 agarose beads (Sigma) according to the manufacturer's protocols.

IMMUNOPRECIPITATION AND IMMUNOBLOT ANALYSIS

Cells were lysed in IP buffer (100 mM Tris–HCl, 100 mM NaCl, pH 7.4, 0.5% Triton X-100, 0.5 mM $CaCl_2$, plus Complete protease inhibitor cocktail, EDTA free) at 4°C for 15 min. Extracts were clarified by centrifugation at 13,000*g* for 20 min, and soluble lysates were pre-cleared with protein G Sepharose (GE Healthcare). The samples were incubated with anti-FLAG M2 agarose (Sigma) and rotated at 4°C for 5 h. The beads were washed five times with IP buffer, and bound proteins were eluted with Laemmli sample buffer. Samples were separated by 10% SDS–PAGE. Immunoblot analysis was performed essentially as described previously [Harris et al., 1999]. The membrane was visualized with SuperSignal West Pico Chemiluminescent Substrate (Pierce, Rockford, IL).

IN VIVO UBIQUITYLATION ASSAY

In vivo ubiquitylation assays were performed essentially as described previously [Shirakura et al., 2007]. Where indicated, cells were treated with 25 μM MG132 (Calbiochem) or with dimethylsulfoxide (DMSO; control) for 30 min prior to collection. FLAG-annexin A1 was immunoprecipitated with anti-FLAG MAb. Immunoprecipitates were analyzed by immunoblotting, using either anti-HA PAb or anti-annexin A1 MAb to detect ubiquitylated annexin A1.

IN VITRO UBIQUITYLATION ASSAY

In vitro ubiquitylation assays were performed essentially as described previously [Shirakura et al., 2007]. For in vitro ubiquitylation of annexin A1, purified GST-annexin A1 was used as a substrate. Purified GST was used as a negative control. Assays were done in 40-μl volumes containing 20 mM Tris–HCl, pH 7.6, 50 mM NaCl, 5 mM ATP, 8 μg of bovine ubiquitin (Sigma), 0.1 mM DTT, 200 ng of mouse E1, 200 ng of E2 (UbcH7), and 0.5 μg of MEF-E6AP, in the presence or absence of $CaCl_2$ as indicated. The reaction mixtures were incubated at 37°C for 120 min followed by immunoblotting.

SIRNA TRANSFECTION

HEK 293T cells (3×10^5 cells in a 6-well plate) were transfected with 40 pmol of either E6AP-specific small interfering RNA (siRNA; Sigma), or scramble negative-control siRNA duplexes (Sigma) using HiPerFect transfection reagent (Qiagen) following the manufacturer's instructions. The E6AP-siRNA target sequences were as follows:

siE6AP-1 (sense) 5′-GGGUCUACACCAGAUUGCUTT-3′; scramble negative control (siCont-1) (sense) 5′-UUGCGGGUCUAAUCACCGATT-3′ [Shirakura et al., 2007]; E6AP-2 (sense), 5′-CAACUCCUGCUCUGAGAUATT-3′; and scramble negative control (siCont-2), 5′-AGACCUACCCGAUUACUGUTT-3′ [Kelley et al., 2005].

ANNEXIN A1 PROTEIN AND E6AP-BINDING ASSAYS

To map the E6AP binding site on annexin A1 protein, GST pull-down assays were performed. A series of recombinant GST-annexin A1 proteins were expressed in *E. coli* and purified using glutathione-Sepharose 4B beads. Equivalent amounts of purified proteins, as estimated by CBB staining, were used for the binding assays. For pull-down assays, purified MEF-E6AP was incubated with GST-annexin A1 proteins immobilized on glutathione-Sepharose 4B beads in 1 ml of the binding buffer (50 mM Tris–HCl [pH 7.4], 150 mM NaCl, 1% Triton X-100, and 5 mM $CaCl_2$) at 4°C for 4 h. The beads were washed four times with binding buffer, and the pull-down complexes were separated by SDS–PAGE on 10% polyacrylamide gels and analyzed by immunoblotting with anti-FLAG MAb.

CYCLOHEXIMIDE (CHX) HALF-LIFE EXPERIMENTS

To examine the half-life of annexin A1 protein, transfected HEK 293T cells were treated with 50 μg/ml CHX at 44 h post-transfection. The cells at time-point zero were harvested immediately after treatment with CHX. Subsequent time points were incubated in medium containing CHX at 37°C for 3, 6, and 9 h as indicated.

CONFOCAL IMMUNOFLUORESCENCE MICROSCOPY

Cells were transfected with pCAG-HA-E6AP C-A and pCAG annexin A1-FLAG using TransIT-LT1 (Takara) according to the manufacturer's instructions. Transfected cells grown on collagen-coated coverslips were washed with PBS, fixed with 4% paraformaldehyde for 30 min at 4°C, and permeabilized with PBS containing 2% FCS and 0.3% Triton X-100. Cells were incubated with anti-HA mouse MAb and anti-FLAG rabbit PAb as primary antibodies, washed, and incubated with Alexa Fluor 488 goat anti-mouse IgG (Molecular Probes, Eugene, OR) and Alexa 555 Fluor goat anti-rabbit IgG (Molecular Probes) as secondary antibodies. Then the cells were washed with PBS, mounted on glass slides, and examined with an LSM510 laser scanning confocal microscope (Carl Zeiss, Oberkochen, Germany).

RESULTS

IDENTIFICATION OF ANNEXIN A1 AS A BINDING PARTNER FOR E6AP

To identify novel substrates for E6AP, we screened for E6AP-binding proteins using pull-down experiments with GST-E6AP. Whole cell lysates from C33-A cells were prepared as described above and incubated with immobilized GST-E6AP or GST alone. After the separation of bound proteins by SDS–PAGE, CBB staining of the gels revealed at least 15 specific bands precipitating with the GST-E6AP. The protein bands were excised from the gel and subjected to in-gel trypsin digestion. The tryptic peptide mixtures were analyzed by MALDI-TOF/MS as described above. Masses obtained using MALDI-TOF were analyzed using the MS-Fit program. This procedure identified seven individual proteins (Fig. 1A,a–g), such as a heat shock protein and a translation elongation factor. One of these bands, migrating at 37 kDa (Fig. 1A,e), was identified as annexin A1 based on six independent MS spectra (Fig. 1B). To verify the interaction of annexin A1 with E6AP, we repeated the pull-down experiments by incubating immobilized GST-E6AP with lysate from C-33A cells. Immunoblot analysis confirmed the proteomic identification of annexin A1 (Fig. 1C).

IN VIVO INTERACTION BETWEEN ANNEXIN A1 AND E6AP

To determine whether the interaction between annexin A1 and E6AP could take place in vivo, annexin A1-FLAG expression plasmid was introduced into HEK 293T cells together with either HA-E6AP expression plasmid or HA-Nedd4 (another HECT domain ubiquitin ligase) [Staub et al., 1996] expression plasmid. A catalytically inactive form of E6AP in which the active site cysteine residue has been substituted with alanine (C843A) was used to avoid potential degradation of interacting proteins. Cells were lysed and annexin A1-FLAG was immunoprecipitated with FLAG-beads. As shown in Figure 2A, HA-E6AP but not HA-Nedd4 was co-immunoprecipitated with annexin A1-FLAG, indicating that E6AP actually interacts with annexin A1 in the cells. We confirmed that the active form of HA-E6AP was also coimmunoprecipitated with annexin A1-FLAG (data not shown).

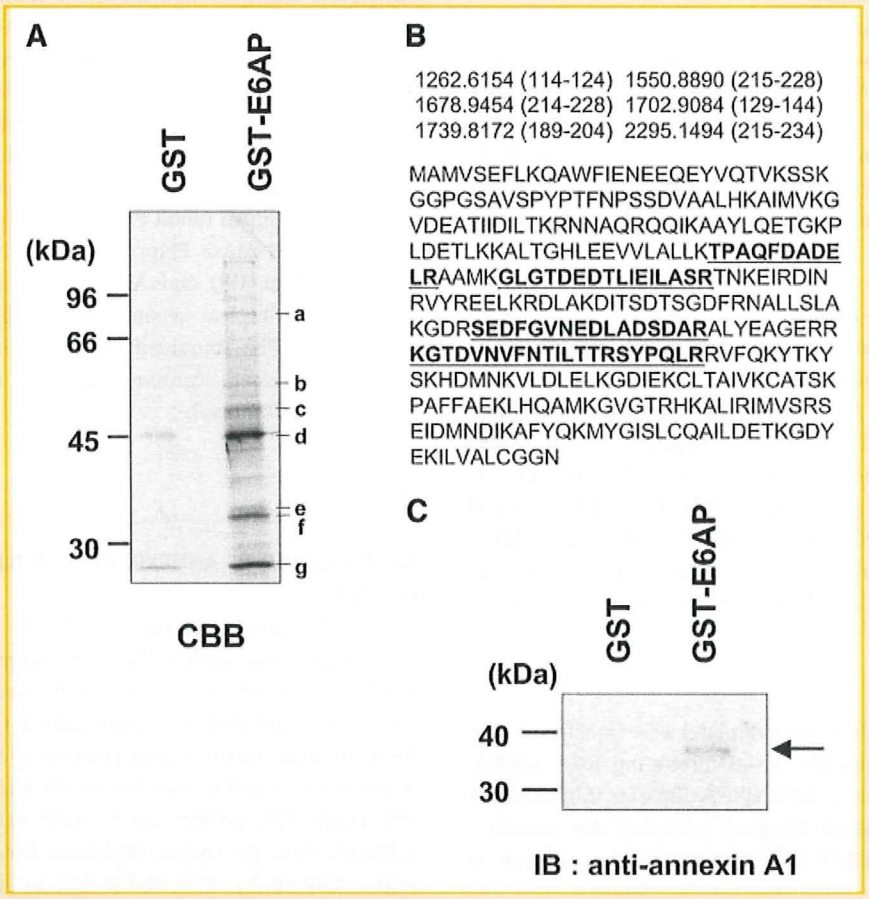

Fig. 1. Identification of annexin A1 as a binding partner for the E6AP. A: GST-E6AP on glutathione-Sepharose beads was incubated with whole-cell extract from C-33A cells. Bound proteins were detected by SDS-PAGE and CBB staining. Molecular weight markers are indicated, as well as the position of p37 (e), which likely corresponds to annexin A1. B: Peptide masses were identified by MALDI-TOF/MS and corresponding amino acids of annexin A1 (trypsin cleavage). Annexin A1 (accession no. 12654863) was identified through MALDI-TOF/MS as a candidate protein interacting with GST-E6AP. The database-fitting program MS-Fit was used to interpret the MS spectra of the protein digests. Six out of 22 masses obtained through the MALDI-TOF analysis corresponded to the theoretical values for annexin A1 cleavage (upper panel, amino acids corresponding to tryptic fragments in brackets) and represented 18% of the proteins' fragments (lower panel, peptides in bold print). The molecular weight search score, MOWSE, was 3.94E + 03. C: The identity of the band shown in panel A as annexin A1 was confirmed by Western blotting with anti-annexin A1 mouse MAb.

To determine whether annexin A1 and E6AP co-localize in the cells, immunofluorescence microscopy analysis was performed in two different cell lines, HEK 293T cells and C-33A cells. The immunofluorescence study showed that E6AP partially co-localized with annexin A1 in the cytoplasm of both types of cells (Fig. 2B).

To determine whether endogenous E6AP interacts with endogenous annexin A1 in vivo, C-33A cells were lysed and subjected to immunoprecipitation with anti-annexin A1 antibody or anti-E6AP antibody. Endogenous E6AP was co-immunoprecipitated with anti-annexin A1 antibody, but not with control antibody (Fig. 2C, left panel, upper lane). Moreover, endogenous annexin A1 was co-immunoprecipitated with anti-E6AP antibody, but not with control antibody (Fig. 2C, right panel, lower lane). These results suggest that endogenous E6AP can interact with endogenous annexin A1 in C-33A cells.

E6AP DECREASES STEADY-STATE LEVELS OF ANNEXIN A1 PROTEIN

To determine whether E6AP functions as an E3 ubiquitin ligase for the ubiquitylation of annexin A1, we assessed the effects of E6AP on annexin A1 protein in HEK 293T cells. The annexin A1-FLAG expression plasmid together with the plasmid for HA-tagged wild-type E6AP, catalytically inactive mutant E6AP, E6AP C-A, or Nedd4, was introduced into HEK 293T cells, and the levels of annexin A1 proteins were examined by immunoblotting. The steady-state levels of annexin A1 protein decreased with an increase of the E6AP plasmids (Fig. 3A,B). However, neither E6AP C-A nor Nedd4 decreased the steady-state levels of the annexin A1 protein, suggesting that E6AP enhances the degradation of annexin A1 protein.

E6AP ENHANCES THE DEGRADATION OF ANNEXIN A1 PROTEIN

To determine whether the E6AP-induced reduction of the annexin A1 protein is due to an increase in the rate of degradation of annexin A1 protein, we examined the degradation of annexin A1 using the protein synthesis inhibitor CHX. Annexin A1 together with wild-type E6AP or inactive mutant E6AP C-A was expressed in HEK 293T cells. At 44 h after transfection, the cells were treated with either 50 μg/ml CHX alone or 50 μg/ml CHX plus 25μM MG132 to inhibit

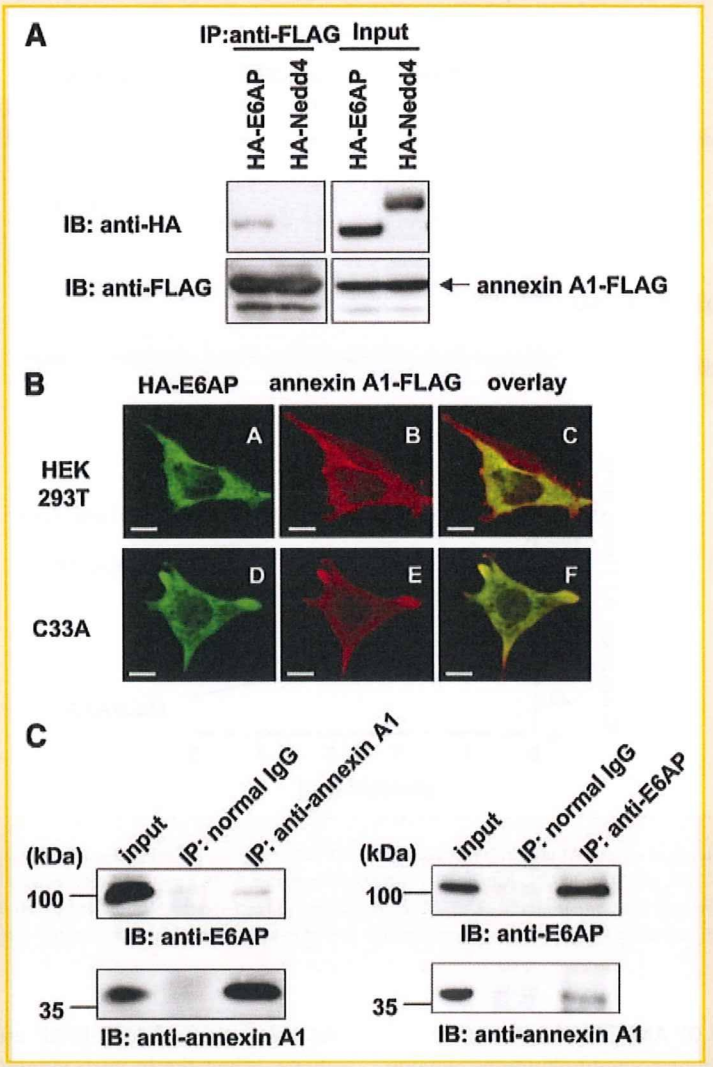

Fig. 2. In vivo interaction between annexin A1 and E6AP. A: HEK 293T cells were co-transfected with pCAG-annexin A1-FLAG together with pCAG-HA-E6AP C-A or pCAG-HA-Nedd4. The cell lysates were immunoprecipitated with FLAG beads and analyzed by immunoblotting with anti-HA PAb or anti-FLAG PAb. B: HEK 293T cells and C-33A cells were transfected with either HA-E6AP plasmid or annexin A1-FLAG plasmid, grown on coverslips, fixed, and processed for double-label immunofluorescence for HA-E6AP or annexin A1-FLAG. All the samples were examined with an LSM510 laser scanning confocal microscope (bar, 10 μm). C: C33A cells were lysed in the cell lysis buffer. The cell lysates were immunoprecipitated with anti-annexin A1 mouse MAb or control normal mouse IgG and analyzed with anti-E6AP mouse mAb or anti-annexin A1 mouse MAb as indicated (left panel). The cell lysates were immunoprecipitated with anti-E6AP mouse mAb or control normal mouse IgG and analyzed with anti-E6AP mouse mAb or anti-annexin A1 mouse mAb as indicated (right panel).

proteasome function. Cells were collected at 0, 3, 6, and 9 h following the treatment and analyzed by immunoblotting (Fig. 4A). Overexpression of E6AP resulted in rapid degradation of the annexin A1 protein, whereas the annexin A1 protein was stable in the cells transfected with inactive mutant E6AP C-A. Treatment of the cells with MG132 inhibited the degradation of annexin A1 (Fig. 4A). These results suggest that E6AP enhances proteasomal degradation of annexin A1.

KNOCKDOWN OF ENDOGENOUS E6AP BY SIRNA RESULTS IN ACCUMULATION OF ENDOGENOUS ANNEXIN A1 PROTEIN

To determine whether or not E6AP is critical for the degradation of endogenous annexin A1 protein, the expression of E6AP was knocked down by siRNA and the expression of annexin A1 and E6AP was analyzed by immunoblotting. We used two different siE6AP duplexes, siE6AP-1 and siE6AP-2, to knockdown the endogenous E6AP. Transfection of either siE6AP-1 or siE6AP-2 into HEK 293T cells resulted in a decrease in E6AP levels by 70–95% (Fig. 4B, the first panel), indicating that both siRNAs against E6AP resulted in a remarkable decrease in the protein level of E6AP. Knockdown of endogenous E6AP resulted in an accumulation of the endogenous annexin A1 protein, but no accumulation of the endogenous annexin A2 protein (Fig. 4B, the second and third panels), suggesting that the ubiquitylation and degradation of endogenous annexin A1 is specifically inhibited by knockdown of endogenous E6AP in vivo. These results suggest that endogenous E6AP plays a role in the proteolysis of endogenous annexin A1.

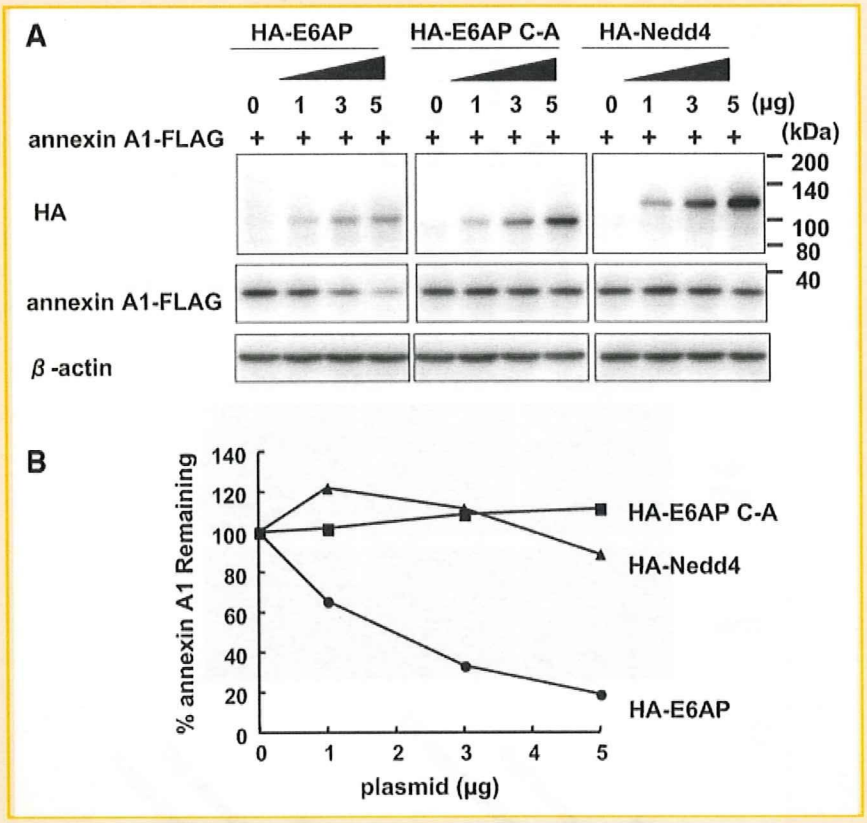

Fig. 3. E6AP decreases steady-state levels of annexin A1 protein in HEK 293T cells. HEK 293T cells (1×10^6 cells/10-cm dish) were transfected with 1 μg of pCAG annexin A1-FLAG along with either pCAG-HA-E6AP, pCAG-HA-E6AP C-A, or pCAG-HA-Nedd4 as indicated. At 48 h post-transfection, protein extracts were separated by SDS-PAGE and analyzed by immunoblotting with anti-HA PAb (top panel), anti-FLAG MAb (middle panel), and anti-β-actin MAb (bottom panel). B: Quantitation of data shown in panel A. Intensities of the gel bands were quantitated using the NIH Image 1.62 program. The level of β-actin served as a loading control. Circles, E6AP; squares, E6AP C-A; triangles, Nedd4.

E6AP MEDIATES UBIQUITYLATION OF ANNEXIN A1 IN VIVO

To determine whether E6AP can induce ubiquitylation of annexin A1 in cells, we performed in vivo ubiquitylation assays. HEK 293T cells were transfected with annexin A1-FLAG plasmid and either E6AP or Nedd4 plasmid, together with a plasmid encoding HA-tagged ubiquitin to facilitate the detection of ubiquitylated annexin A1 protein. Cell lysates were immunoprecipitated with anti-FLAG MAb and immunoblotted with anti-HA PAb to detect ubiquitylated annexin A1 protein. Only a faint ubiquitin signal was detected in the cells co-transfected with empty plasmid or Nedd4 plasmid (Fig. 5A, lanes 4 and 6). In contrast, co-expression of E6AP led to readily detectable ubiquitylated forms of the annexin A1 as a smear of higher-molecular-weight bands (Fig. 5A, lane 5). Immunoblot analysis with anti-FLAG PAb confirmed that annexin A1-FLAG proteins were immunoprecipitated and that higher-molecular-weight bands conjugated with HA-ubiquitin were indeed ubiquitylated forms of the annexin A1 proteins (Fig. 5B, lane 5). These results suggest that E6AP enhances ubiquitylation of annexin A1 in the cells.

E6AP MEDIATES UBIQUITYLATION OF ANNEXIN A1 IN VITRO

To reconstitute the E6AP-mediated ubiquitylation of annexin A1 in vitro, we performed an in vitro ubiquitylation assay of the annexin A1 using purified MEF-E6AP and GST-annexin A1 as described above. When the in vitro ubiquitylation reaction was carried out either in the absence of MEF-E6AP or in the presence of MEF-E6AP C-A, no ubiquitylation signal was detected (Fig. 5C, lanes 4 and 5). However, inclusion of purified MEF-E6AP in the reaction mixture resulted in ubiquitylation of GST-annexin A1 (Fig. 5C, lane 6), while no ubiquitylation was observed in the absence of ATP (Fig. 5C, lane 7). No signal was detected when GST was used as a substrate (data not shown). These results indicate that E6AP directly mediates ubiquitylation of annexin A1 protein in an ATP-dependent manner.

Ca^{2+}-DEPENDENT INTERACTION BETWEEN ANNEXIN A1 AND E6AP

We next assessed the effects of Ca^{2+} on the interaction between annexin A1 and E6AP. We performed the pull-down experiments by incubating immobilized GST-E6AP or GST alone with purified His-tagged annexin A1 in the presence or absence of 1 mM $CaCl_2$. After precipitation and SDS-PAGE, the bound annexin A1 was detected by immunoblotting with anti-annexin A1 antibody. GST-E6AP, but not GST, was able to precipitate annexin A1 only in the presence of Ca^{2+} (Fig. 6A, lane 4). These interactions were dependent on the concentration of Ca^{2+}, as increasing concentrations of Ca^{2+} resulted in an increase of binding of annexin A1 to E6AP (Fig. 6B). These

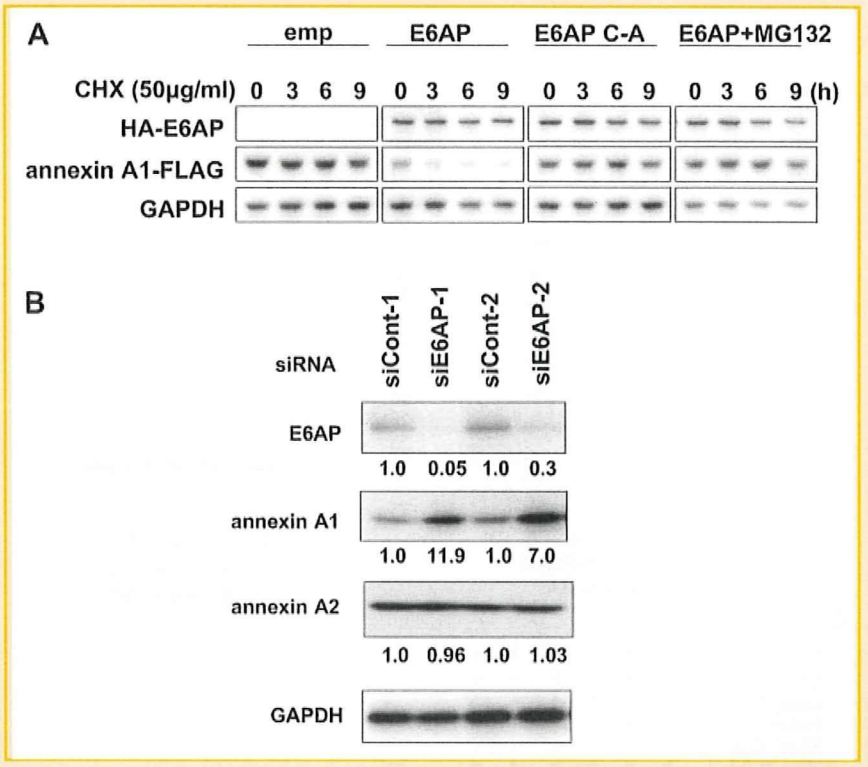

Fig. 4. E6AP-dependent degradation of annexin A1 protein. A: HEK 293T cells (1×10^6 cells/10-cm dish) were transfected with 1 μg of pCAG-annexin A1-FLAG plus 4 μg of empty vector, pCAG-HA-E6AP, or pCAG-HA-E6AP C-A. The cells were treated with 50 μg/ml CHX at 44 h after transfection. Cell extracts were collected at 0, 3, 6, and 9 h after treatment with CHX, followed by immunoblotting. Data are representative of three independent experimental determinations. B: Knockdown of endogenous E6AP by siRNA resulted in the accumulation of endogenous annexin A1 in HEK 293T cells. HEK 293T cells (3×10^5 cells/6-well plate) were transfected with 40 pmol of E6AP-specific duplex siRNA (or scramble negative control). Two sets of siRNAs (siE6AP-1 and siCont-1, siE6AP-2 and siCont-2) were used as described in Materials and Methods Section. The cells were harvested at 120 h after siRNA transfection. The relative levels of protein expression were quantitated using the NIH Image 1.62 program and are indicated below in the respective lanes. Data are representative of three independent experimental determinations.

results indicate that E6AP binds annexin A1 in a Ca^{2+}-dependent manner.

UBIQUITYLATION OF ANNEXIN A1 BY E6AP IS CA^{2+}-DEPENDENT

The HECT-type ubiquitin ligases transfer ubiquitin molecules to the substrates through direct interaction. Therefore, the E6AP-annexin A1 interaction is considered to be necessary for E6AP-mediated annexin A1 ubiquitylation. To determine if the molecular interaction is required for E6AP-mediated annexin A1 ubiquitylation, we performed in vitro ubiquitylation assay in the presence or absence of 1 mM $CaCl_2$. When in vitro ubiquitylation reaction was carried out in the presence of Ca^{2+}, the higher-molecular-weight species of GST-annexin A1 were detected with anti-GST PAb (Fig. 6C, lane 2), indicating that annexin A1 is polyubiquitylated by E6AP in vitro. However, no ubiquitylation signal was detected when the ubiquitylation reaction was carried out in the absence of Ca^{2+} (Fig. 6C, lane 1), indicating that the E6AP-annexin A1 interaction is required for E6AP-mediated annexin A1 ubiquitylation.

To further investigate whether the ubiquitylation of annexin A1 is dependent on the presence of Ca^{2+}, we examined the effects of EGTA on the E6AP-mediated ubiquitylation of annexin A1. Polyubiquitin chains were synthesized even in the presence of a high concentration of EGTA (Fig. 6D), indicating that E6AP was active even in the presence of EGTA. However, increasing amounts of EGTA resulted in decreases in the ubiquitylation of annexin A1 (Fig. 6E), suggesting that chelating the Ca^{2+} in the reaction mixture with EGTA inhibits the ubiquitylation of annexin A1. These findings suggest that the ubiquitylation of annexin A1 by E6AP is dependent on the presence of Ca^{2+}.

E6AP-BINDING DOMAIN FOR ANNEXIN A1 PROTEIN

To map the E6AP-binding domain on annexin A1 protein, GST pull-down assays were performed using a panel of annexin A1 deletion mutants expressed as GST-fusion proteins. Figure 7A shows a schematic representation of annexin A1 and known motifs in annexin A1. A series of deletion mutants of annexin A1 as GST fusion proteins (Fig. 7A) were expressed in *E. coli*. Purified MEF-E6AP was used to determine E6AP-binding domain. GST pull-down assays revealed that the core domain of annexin A1 (42-346), but not the N-terminal tail of annexin A1 (1-41), bound to E6AP (Fig. 7B, lanes 4 and 3). GST pull-down assays also showed that annexin A1 (114-274) and annexin A1 (196-346), but not annexin A1 (42-195), were able to bind to E6AP (Fig. 7B, lanes 5-7). As shown in Fig. 7C, GST-annexin A1 (196-274) bound to E6AP. These findings suggest that annexin repeat domain III is important for E6AP binding.